National Science Foundation
MARGINS Program

Central America Tectonics Workshop
Costa Rica - July 2001

Quaternary neotectonics of the Costa Rican coastal fore arc

Field Trip Guide

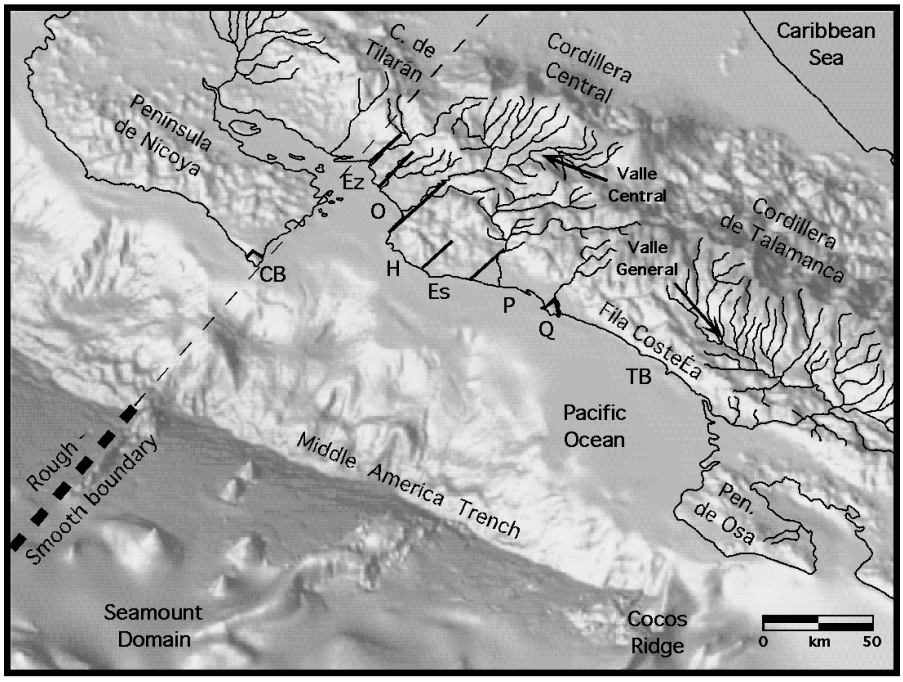

Jeffrey S. Marshall Cal Poly University, Pomona, California

Thomas W. Gardner Trinity University, San Antonio, Texas

Donald M. Fisher Penn State, University Park, Pennsylvania

Peter B. Sak Penn State, University Park, Pennsylvania

J. Marino Protti OVSICORI-UNA, Heredia, Costa Rica.

Quaternary neotectonics of the Costa Rican coastal fore arc

Field Trip Guide

J.S. Marshall, T.W. Gardner, D.M. Fisher, P.B. Sak, and J.M. Protti

email: marshall@csupomona.edu

Table of Contents

Field Trip Itinerary

7/4 WED.
Arrive airport. Lodging at Hotel Aeropuerto, Alajuela

7/5 THUR.

6:30-7:30	Breakfast at hotel
7:30-8:00	Meet & board bus in parking lot of Hotel Aeropuerto
8:00-10:00	Drive Inter American highway to Puntarenas ferry dock
10:00-12:30	Ferry ride to Paquera, lunch
12:30-2:00	Drive to Tango Mar Hotel
2:00-3:00	Check in to hotel. (High Tide: 2:45)
3:00-6:00	Tango Mar beach - Nicoya Complex/Slope sediment unconformity, Holocene shore platforms, beach waterfall, swimming (Sunset: 6:04)
7:00-8:30	Dinner & cocktails on beach (Low Tide: 9:03)

7/6 FRI.

6:00-8:00	Breakfast at hotel, check out, load bus. (Sunrise: 5:23)
8:00-9:30	Drive to Cabuya (southern tip of Península de Nicoya) (Low Tide: 9:15)
9:30-10:00	Cabuya shore platform/Isla Cabuya - rapid uplift above subducting seamounts, marine terrace genesis, deformed Paleogene slope sediments.
10:00-12:00	Holocene Cabuya terrace - walk across terrace & up to Pleistocene Cobano terrace, dated terrace deposits, coastal uplift rates, view of Cabo Blanco area
12:00-1:00	Cabo Blanco visitor's center - bag lunch on cliffs, Nicoya earthquake cycle.
1:00-3:00	Drive to ferry dock
3:00-6:00	Ferry ride to Puntarenas (High Tide: 3:28)
6:00-7:30	Drive to Villa Lapas (Sunset: 6:04)
7:30-9:30	Arrive Villa Lapas. Check in. Dinner.

7/7 SAT.

7:00-8:00	Breakfast at hotel (Sunrise: 5:23)
8:00-9:00	Río Tarcoles bridge - Fluvial terraces, Tárcoles fault, & crocodiles!
9:00-10:00	Bajamar coastal cliffs - lahar framework of Orotina debris fan. (Low Tide: 9:56)
10:00-11:00	Jesús María quarry - Snake Flow welded tuff: Ar/Ar dated timeline & link between Quaternary volcanics of coastal plain & Valle Central
11:00-11:30	Jesús María fault scarp and mesoscale faults in Miocene sediments
11:30-12:30	Alto de las Mesas overlook - overview of Orotina debris fan & fore arc fault blocks: Esparza, Orotina, Herradura (moderate, low, & high uplift rates)
12:30-2:00	Mata de Limón - seafood lunch along mangrove estuary
2:00-3:30	Río Barranca fluvial terraces, El Diablo surface, & Barranca fault
3:30-4:30	Return to Villa Lapas
5:00-7:30	Swimming pool. Sunset happy hour. Dinner. (Sunset: 6:04)
8:00-9:00	Evening presentation/discussion in meeting room.

7/8 SUN.

7:00-8:00	Breakfast at hotel (Sunrise: 5:24)
8:00-9:00	Pta. Guapinol (Jaco) - Herradura block, Nicoya complex outcrops, & coastal view
9:00-12:00	Punta Judas shore platform - faults & marine terraces, lunch (Low Tide: 10:37)
12:00-1:30	Parrita/Alto Guapinol overlook: fluvial terraces, Esterillos, Parrita & Quepos blocks
1:30-3:30	Villa Caletas overlook: Summary view of entire central coast & Golfo de Nicoya
3:30-5:30	Return to Valle Central, arrive Hotel La Contesa, Heredia (Sunset: 6:04)

NSF MARGINS Program
Central America Tectonics Workshop Field Trip:
Costa Rica - July 2001

Quaternary neotectonics of the Costa Rican coastal fore arc

Jeffrey S. Marshall, Geological Sciences Dept., Cal Poly Pomona, CA, 91768

Thomas W. Gardner, Dept. of Geosciences, Trinity University, San Antonio, TX, 78212.

Donald M. Fisher, Dept. of Geosciences, Penn State University, University Park, PA, 16802.

Peter B. Sak, Dept. of Geosciences, Penn State University, University Park, PA, 16802.

J. Marino Protti, OVSICORI, Universidad Nacional, Heredia, Costa Rica.

Introduction

Along convergent margins, fore arc deformation is strongly influenced by the character of the subducting oceanic plate (e.g., Jarrard, 1986; Lajoie, 1986). Such parameters as the convergence rate, slab angle, bathymetric relief, and sediment thickness help to determine a particular style of coastal tectonics. The Pacific margin of southern Central America (Fig. 1) provides an excellent venue for examining the relationship between coastal tectonics and the characteristics of the subducting plate. Along the Middle America Trench, where the Cocos plate subducts beneath the Caribbean plate and Panama block, the oceanic crust exhibits dramatic variations in age, composition, thickness, and roughness. Within less than 500 km, from central Nicaragua to southern Costa Rica (Fig. 1), changing subduction parameters along the Middle America Trench generate sharp contrasts in the style of upper plate deformation (Gardner et al., 1987 and 1992; Fisher et al., 1994 and 1998; von Huene et al., 1995 and 2000; Marshall et al., 2000).

On this field trip, we will explore the Quaternary geology and geomorphology of the coastal fore arc region of central Costa Rica (Fig. 2). We will see how the inner fore arc crust deforms in response to incoming sea-floor roughness on the Cocos plate and look at how changes in subduction have influenced landscape evolution in the coastal zone. The distribution of marine and fluvial terraces and patterns of active faulting provide critical evidence used to evaluate Quaternary uplift rates and to characterize fore-arc kinematics. The overall pattern of uplift and faulting along the central Costa Rican coastline reveal a strong relationship between the kinematics of inner fore-arc deformation and distribution of roughness elements on the subducting Cocos plate.

Costa Rican Pacific Coast: Tectonics and Geomorphology

The Rough-Smooth Boundary and Cocos Ridge

Central Costa Rica (Figs. 1 and 2) has long been recognized as a segment boundary along the Middle America convergent margin (Stoiber and Carr, 1973; Carr, 1976; Burbach et al., 1984). Pronounced changes in arc volcanism, subduction zone seismicity, and fore arc structure occur across the central Costa Rican portion of the Middle America Trench (e.g., Güendel, 1986; Protti, 1991 and 1994; Malavassi, 1991; Gardner et al., 1987 and 1992; Fisher et al., 1994 and 1998; de Boer et al., 1995; Kolarsky et al., 1995; Protti et al., 1995; von Huene et al., 1995 and 2000; Marshall, 2000; Marshall et al., 2000). The southern tip of the Península de Nicoya (Fig. 3, site 11) and the Orotina-Esparza coastal plain southeast of Puntarenas (Fig. 3, sites 3-5) lie along the onland projection of the "rough-smooth boundary" (Hey, 1977) on the subducting Cocos plate (Figs. 2 and 3). This morphologic lineament separates smooth, low-relief oceanic crust to the NW, and rough, high-relief crust to the SE (von Huene et al., 1995). The trend of this feature coincides with a contortion in the Benioff zone (Protti et al., 1995), the northern edge of a volcanic gap (de Boer et al., 1995), faulting across the volcanic arc (Marshall et al., 2000), and sharp contrasts in coastal tectonics in the overriding fore arc (Gardner et al., 1992; Fisher et al., 1998).

Prominent bathymetric features on the rough domain include the aseismic Cocos Ridge, the Quepos plateau, and the Fisher seamount chain, all products of hotspot volcanism along the Galapagos Rift (Fig. 1; Holden and Dietz, 1972; von Huene et al., 1995 and 2000; Barckhausen et al., 1998; Meschede et al., 1998; Stavenhagen et al., 1998; Werner et al., 1999). The Cocos Ridge began subducting sometime in the late Neogene (Collins et al., 1995; Kolarsky et al., 1995; Meschede et al., 1999b), flattening the subducting slab (Protti et al., 1995) and extinguishing arc volcanism in southern Costa Rica (de Boer et al., 1995). Rapid uplift and shortening in the overriding crust extend through the volcanic arc from the fore arc Península de Osa and Terraba belt to the back arc Limón belt (Fig. 2; Corrigan et al., 1990; Gardner et al., 1992; Montero, 1994; Bullard, 1995; Collins et al., 1995; Kolarsky et al., 1995).

Along the central Costa Rican coast, NW of the Cocos Ridge, the pronounced impact of ridge indentation diminishes (Gardner et al., 1992). Subducting seamounts on the NW ridge flank (Figs. 2 and 3), deform the outer trench slope (von Huene et al., 1995 and 2000; Barckhausen et al., 1998) and produce differential uplift of coastal fault blocks (Fig. 3; Marshall and Anderson, 1995; Fisher et al., 1998; Gardner et al, 2001). Subhorizontal subduction of hotspot thickened crust in this area drives active faulting within a deformation front across the volcanic arc (Fig. 2; CCRDB of Marshall et al., 2000). Slab flattening and trench retreat by fore arc erosion (e.g., Meschede et al., 1999a; Vannuchi et al., 2000), may have led to northeastward migration of the volcanic arc from the extinct Cordillera de Aguacate to the modern Cordillera Central (Fig. 2; Marshall, 2000).

Coastal Tectonics

The distribution of Quaternary uplift along the Costa Rican Pacific coast is primarily controlled by the subducting bathymetric relief on the thinly sedimented Cocos plate (Gardner et al., 1992; Marshall and Anderson, 1995; Fisher, et al., 1994 and 1998). Nearly orthogonal convergence (10 cm/yr) focuses the tectonic impact of ridges and linear seamount chains on discrete segments of the coastline for extended periods of time (Figs. 2 and 3). Quaternary uplift rates derived from radiometrically dated marine and fluvial terraces mirror the offshore distribution of these bathymetric features (Wells et al., 1988; Gardner et al., 1992, Marshall and Anderson, 1995; Fisher et al., 1994 and 1998; Marshall, 2000; Gardner et al, 2001).

Over the past two decades, a series of investigations have examined Quaternary terraces along the Pacific margin of Costa Rica (Fig. 3). Several of these studies present a broad overview of regional coastal tectonics (e.g., Fischer, 1980; Battistini and Bergoeing, 1983; Gardner et al., 1987 and 1992; Wells et al., 1988; Fisher et al., 1994 and 1998). Others focus on localized flights of terraces along discrete segments of coastline (Mora, 1985; Hare and Gardner, 1985; Pinter, 1988; Drake, 1989; Marshall, 1991; Marshall and Anderson, 1995; Bullard, 1995; Pazzaglia et al., 1998; Sak, 1999; Marshall, 2000; Gardner et al., 2001). Recent work has expanded coastal terrace studies northward into Nicaragua (Gerth et al., 1999; Gerth, 2000; Marshall, 2000).

In general, Quaternary uplift rates decrease parallel to the margin, moving northwestward away from the subducting Cocos Ridge (Figs. 2 and 3; Gardner et al., 1992). These rates range from a maximum of 6-7 m/k.y. astride the ridge in the south (Fig. 3; site 10) to background rates of 1-2 m/k.y. above smooth subducting crust in the north (Fig. 3; NW of site 11). This overall long-wavelength trend reflects a decrease in upward flexure of the overriding crust as the thickness of the subducting plate diminishes away from the ridge axis (Gardner et al., 1992). Shorter-wavelength roughness related to seamounts superimposes local variability on this background uplift pattern (Fisher et al., 1998). Along the central Costa Rican Pacific coast, uplift rates vary sharply across a series of margin-perpendicular faults that segment the coastal fore arc into discrete fault blocks (Fig. 3; Fisher et al., 1994 and 1998; Marshall et al., 2000). Ongoing research (e.g., Marshall, 2000; Gardner et al., 2000; Sak et al., in review) is aimed at developing a regional correlation framework for coastal terraces to provide better constraints on the distribution of Quaternary uplift along the entire Pacific margin of southern Central America.

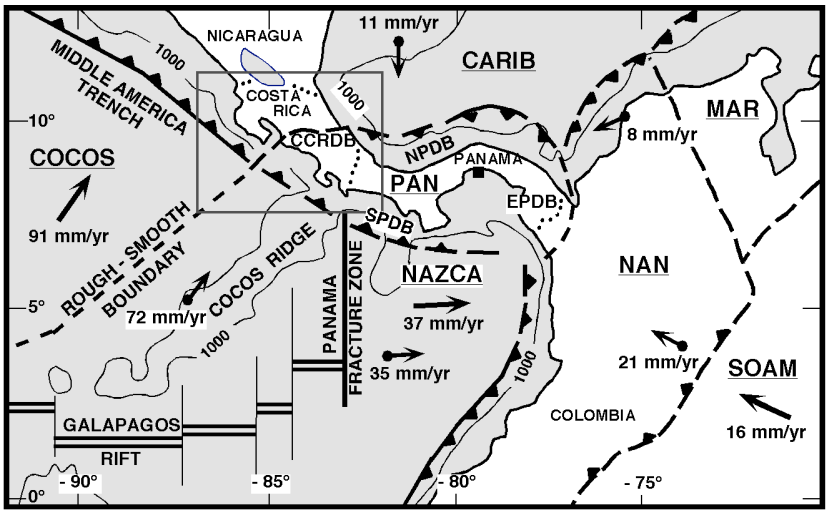

Figure 1. Tectonic setting of southern Central America (from Marshall, 2000). Costa Rica and the Central Costa Rica Deformed Belt (CCRDB) mark the western margin of the Panama block (PAN). The CCRDB links the North Panama Deformed Belt (NPDB) with the Middle America Trench, and is located onshore of the rough-smooth boundary on the subducting Cocos plate (COCOS). Large arrows show modeled plate motions (DeMets et al., 1990) relative to the Caribbean plate (CARIB). Small arrows show velocities for Global Positioning System (GPS) sites (solid circles) relative to Panama (solid square) (Kellogg and Vega, 1995). The Cocos Ridge is outlined by the 1000-m depth contour. The rectangle shows area of Fig. 2. NAZCA, Nazca plate; SOAM, South American plate, MAR; Maracaibo block; NAN, North Andes block; EPDB, East Panama Deformed Belt; SPDB, South Panama Deformed Belt. Map is compiled from Lonsdale and Klitgord (1978), Mackay and Moore (1990), Silver et al. (1990), Kellogg and Vega (1995), Protti et al. (1995), and Westbrook et al. (1995).

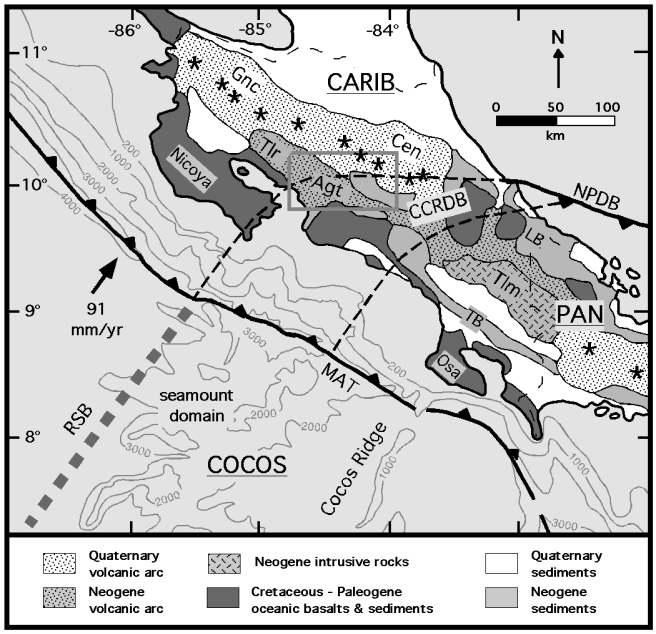

Figure 2. Geologic map of Costa Rica (from Marshall, 2000), showing distribution of major volcanic cordilleras relative to plate boundary faults and offshore bathymetry (contours in meters). The active Quaternary volcanic arc (asterisks) spans the Cordillera de Guanacaste (Gnc) and Cordillera Central (Cen). The extinct Neogene arc includes the Cordillera de Tilarán (Tlr), Cordillera de Aguacate (Agt), and Cordillera de Talamanca (Tlm). The CCRDB (outlined by dashed lines) marks a zone of diffuse faulting between the Panama block and the Caribbean plate (Marshall et al., 2000). The SW limit of active volcanism and the NW limit of the CCRDB align with the rough-smooth boundary (RSB) on the subducting Cocos plate. The RSB separates smooth crust to the NW from rough crust (seamount domain and Cocos Ridge) to the SE. The subducting Cocos Ridge aligns with the volcanic gap and uplifted intrusive rocks of the Cordillera de Talamanca, and with the inverted sedimentary basins of the Terraba thrust belt (TB) and the Limón thrust belt (LB). MAT, Middle America Trench; Nicoya, Península de Nicoya; Osa, Península de Osa. The gray rectangle shows the area of Figs. 4 and 6.

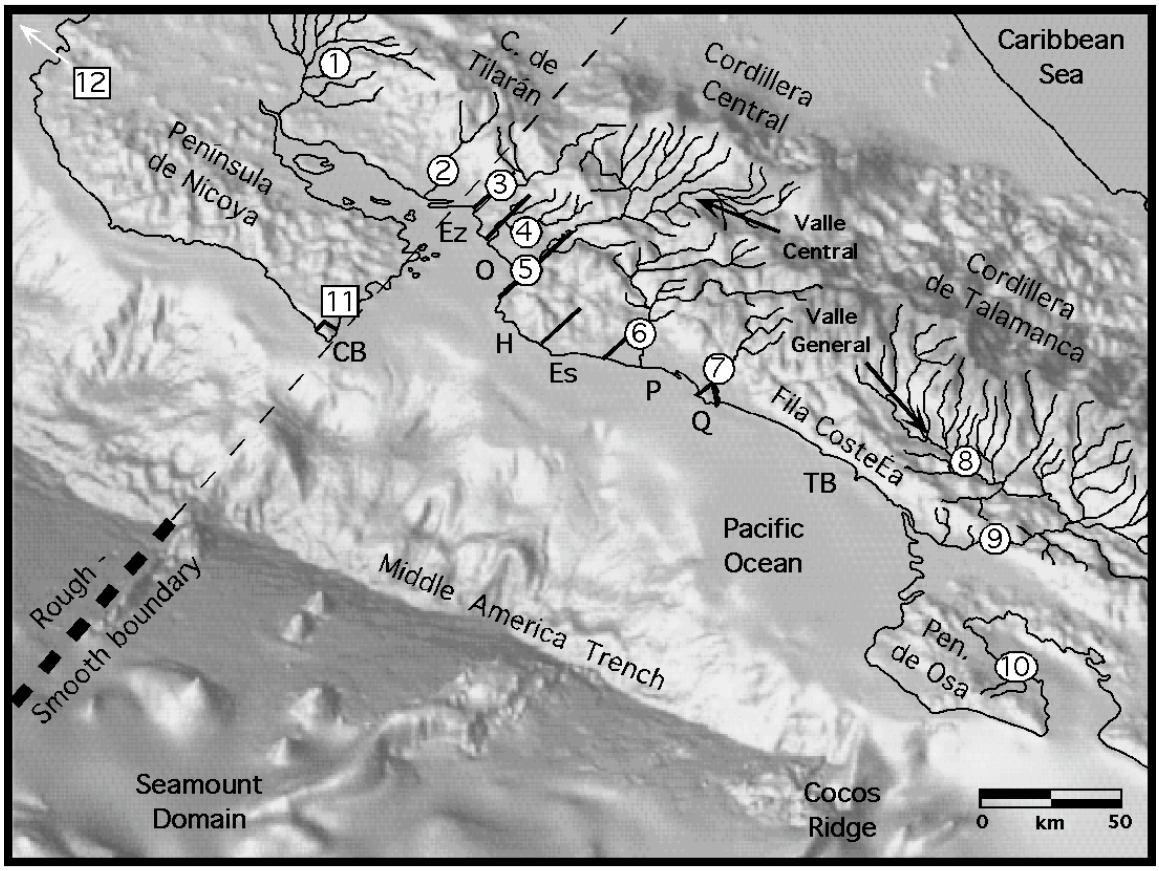

Figure 3. Digital elevation map of Costa Rican Pacific coast (from Marshall, 2000) showing Quaternary terrace study sites, associated drainage networks, and primary tectonic features. Numbered circles indicate fluvial terrace study sites: 1, Río Cañas; 2, Río Aranjuez; 3, Río Barranca; 4, Río Machuca; 5, Río Tárcoles; 6, Río Parrita; 7, Río Naranjo; 8, Río General; 9, Río Terraba; 10, Río Tigre. Numbered boxes show marine terrace study sites: 11, Cobano surface; 12, La Boquita surface (located 140 km NW of upper left corner of figure). Thin dashed line marks the onland projection of the rough-smooth boundary (heavy dashed line) on the subducting Cocos plate. Thick solid lines indicate major block bounding faults of the subaerial fore arc. Fault blocks include: CB, Cabo Blanco; Ez, Esparza; H, Herradura; Es, Esterillos; P, Parrita; Q, Quepos; and TB, Terraba belt. Digital elevation model (gray background) from Fisher et al. (1998).

DAY 1 (morning)

Thursday, 5 July 2001

Landscape evolution of the central Costa Rican volcanic arc and coastal fore arc region

Road Log (Day 1, morning):

During today's leg of the field trip, we will travel from the Valle Central across the extinct Aguacate volcanic range, and then descend the Pacific slope to the port city of Puntarenas. There we will board a ferry and cross the Golfo de Nicoya to the southeastern coast of the Península de Nicoya. We will spend this afternoon and tommorrow morning exploring the structure and geomorphology of the coastal fore arc near the peninsula's southern tip.

We begin our trip heading westward on the Inter-American highway across the broad upland surface of the Valle Central basin (Figs. 3 and 4). This lush highland valley is Costa Rica's cultural and economic heartland, providing a home to nearly half of the country's population in the urban centers of San José, Cartago, Heredia, and Alajuela. Rich volcanic soils support an abundance of Costa Rica's world famous arabica coffee, as well as sugar cane, ornamental plants, and a wide array of other crops.

The Valle Central's relatively low relief landscape surface overlies a thick (>1 km) accumulation of Quaternary pyroclastic rocks, lavas, lahars, and lacustrine sediments (Figs. 4 and 5). The active stratovolcanoes of the Cordillera Central rise above the valley floor to the north (left to right: Platanár, Poás, Barva, Irazú) and the eroding remnants of the extinct Cordillera de Aguacate ring the southern horizon. As we proceed westward, the highway crosses several deep canyons incised into the valley floor by rivers draining toward the deep gorge of the Río Grande de Tárcoles to the southwest (Fig. 3, up stream of site 5). Visible as a large notch cut in the Aguacate volcanic range, the Tárcoles gorge links the Valle Central drainage network with the Orotina debris fan on the central Pacific slope (Fig. 4). We will explore this part of the coast later in the field trip.

Our route continues to the base of the Aguacate cordillera and passes through the prominent bowl-shaped Palmares caldera (Fig. 4), one of the suspected sources of the Valle Central pyroclastic sequence. We then climb over the Aguacate divide and descend toward the Pacific coast through one of Costa Rica's primary gold mining districts (associated with hydrothermal activity in the extinct arc). Near the coast, the highway levels out and crosses the Quaternary El Diablo surface, a broad alluvial fill terrace (Fig. 4, unit Qtl) formed along the lower reaches of the Río Barranca (Fig. 3, site 3). Offest of this terrace demonstrates late Quaternary slip along the Barranca fault. This distinctive terrace can be correlated between drainages along the entire Pacific coast, providing an important means of evaluating the distribution of uplift across inner fore arc fault blocks (Fig. 3). Finally, we turn toward the port city of Puntarenas, built on a remarkable twelve-kilometer long sand spit extending into the mouth of the Golfo de Nicoya.

Geologic Overview (Day 1, morning):

Cenozoic Landscape Evolution of central Costa Rica

The geomorphic evolution of central Costa Rica has been profoundly influenced by changes in Cocos plate subduction during the late Cenozoic. The introduction of hotspot thickened seafloor into the subduction zone initiated a shallowing of the subducting slab and a progressive retreat of the volcanic front from the Cordillera de Aguacate to the Cordillera Central (Fig. 4; Marshall, 2000). This northeastward expansion of the volcanic arc resulted in the formation of the Valle Central basin and a shift in the location of the Pacific-Caribbean drainage divide. Linkage of the Valle Central drainage with the Pacific slope established a pathway for spillover of Quaternary pyroclastic flows onto the Orotina debris fan at the coast (Fig. 4; Marshall, 2000).

The following paragraphs outline a five stage model for late Cenozoic landscape evolution in central Costa Rica (Marshall, 2000). This reconstruction is based on stratigraphic correlations (Figs. 4 and 5) and the first $^{40}Ar/^{39}Ar$ isotopic ages (Fig. 5; Table 1) for young volcanic rocks of the Valle Central and Orotina debris fan (Marshall and Idleman, 1999; Marshall, 2000).

Stage 1 - Miocene to Pliocene. During the Miocene (Fig. 6, stage 1), the original primitive island arc of central Costa Rica evolved toward a composite volcanic cordillera (Kussmaul et al., 1994). Widespread calc-alkaline volcanism built the stratovolcanoes of the Aguacate range and created a drainage divide separating the Pacific Ocean and Caribbean Sea. The $^{40}Ar/^{39}Ar$ ages (Fig. 5; Table 1) for Aguacate Group lavas (TQv) establish activity within the core of the Aguacate range as late as 5.0 Ma (Marshall and Idleman, 1999; Marshall, 2000). Subduction of the Cocos Ridge and seamount domain may have begun shortly after this time (3-4 Ma) in the early Pliocene (Collins et al., 1995; Meschede et al., 1999b)

Stage 2 - Late Pliocene to early Pleistocene. By the late Pliocene (Fig. 6, stage 2), the subducting slab began to flatten beneath central Costa Rica as hotspot-thickened oceanic crust entered the subduction zone. The northward propagation of a deformation front (Central Costa Rica deformed belt) ahead of the shallow slab initiated faulting across the volcanic arc (Marshall et al., 2000). Pyroclastic eruptions and sector collapse within the Cordillera de Aguacate generated extensive volcanic mud flows (TQl - Tivives Fm.; Madrigal, 1970) on the Pacific coast. Repeat emplacement of these lahars built the framework for the Orotina debris fan. The $^{40}Ar/^{39}Ar$ ages (Fig. 5; Table 1) constrain the timing of these events to 1.7 - 1.1 Ma (Marshall and Idleman, 1999; Marshall, 2000).

Stage 3 - Early to Middle Pleistocene. With increased flattening of the subducting slab in the early Pleistocene (Fig. 6, stage 3), the volcanic front migrated into the back arc. Widespread andesite lava flows and ignimbrites (Qv_4 - Intracañon Fm.) were erupted along the Caribbean slope of the Aguacate range (Echandi, 1981; Alvarado, 1985; Denyer and Arias, 1991; Kussmaul et al., 1994). These deposits blocked Caribbean drainages, forming ponded lakes within an early Valle Central basin. The $^{40}Ar/^{39}Ar$ ages (Fig. 5; Table 1) show deposition of the Intracañon Fm. from

760-340 ka (Marshall and Idleman, 1999; Marshall, 2000). Drainage capture across the Aguacate range, and reversal of Valle Central drainages toward the Pacific coast occurred during this period.

Stage 4 - Middle to late Pleistocene. In the middle Pleistocene (Fig. 6, stage 4), caldera eruptions on the flank of the Aguacate range generated silicic ignimbrites (Qv_3 - Avalancha Fm.) that smothered the Valle Central (Echandi, 1981; Alvarado, 1985; Denyer and Arias, 1991; Kussmaul et al., 1994). Westward spillover through the Tárcoles gorge and down to the Pacific slope deposited distal branches of these ash flows (Qv_2 - Orotina Fm.; Madrigal, 1970) across the Orotina debris fan. Meandering paleo-stream channels are preserved across the fan surface as inverted topographic ridges of welded tuff overlying river gravels ("snake flow"). The $^{40}Ar/^{39}Ar$ ages (Fig. 5; Table 1) demonstrate a sudden transition from andesite lavas (Qv_4 - Intracañon Fm.) to andesitic-dacitic ignimbrites (Qv_3 - Avalancha Fm.) at approximately 340 ka (Marshall and Idleman, 1999; Marshall, 2000). The isotopic ages also confirm the correlation between the Qv_3 Electriona member tuff of the Valle Central and the Qv_2 snake flow on the Pacific slope.

Stage 5 - Late Pleistocene to Holocene. By the late Pleistocene (Fig. 6, stage 5), shallow subduction had achieved a steady state beneath central Costa Rica. The modern stratovolcanoes of the Cordillera Central began to develop with the extrusion of basaltic andesite lavas and tephras (Qv_1 - Poás Group; Echandi, 1981; Alvarado, 1985; Denyer and Arias, 1991; Kussmaul et al., 1994). Growth of the Cordillera Central firmly established a new drainage divide and fixed the Valle Central within the Pacific slope drainage. Diffuse faulting within the Central Costa Rica deformed belt (Marshall et al., 2000) extended across the volcanic arc and Valle Central, offsetting many Quaternary volcanic units. On the coastal plain, vertical motion across northeast-trending faults offset Quaternary deposits of the Orotina debris fan (Fisher et al., 1994). Steep, margin-perpendicular faults along the central Costa Rican coast may accommodate differential uplift of fore arc blocks caused by seamount subduction beneath the margin (Fisher et al., 1998; Marshall et al., 2000).

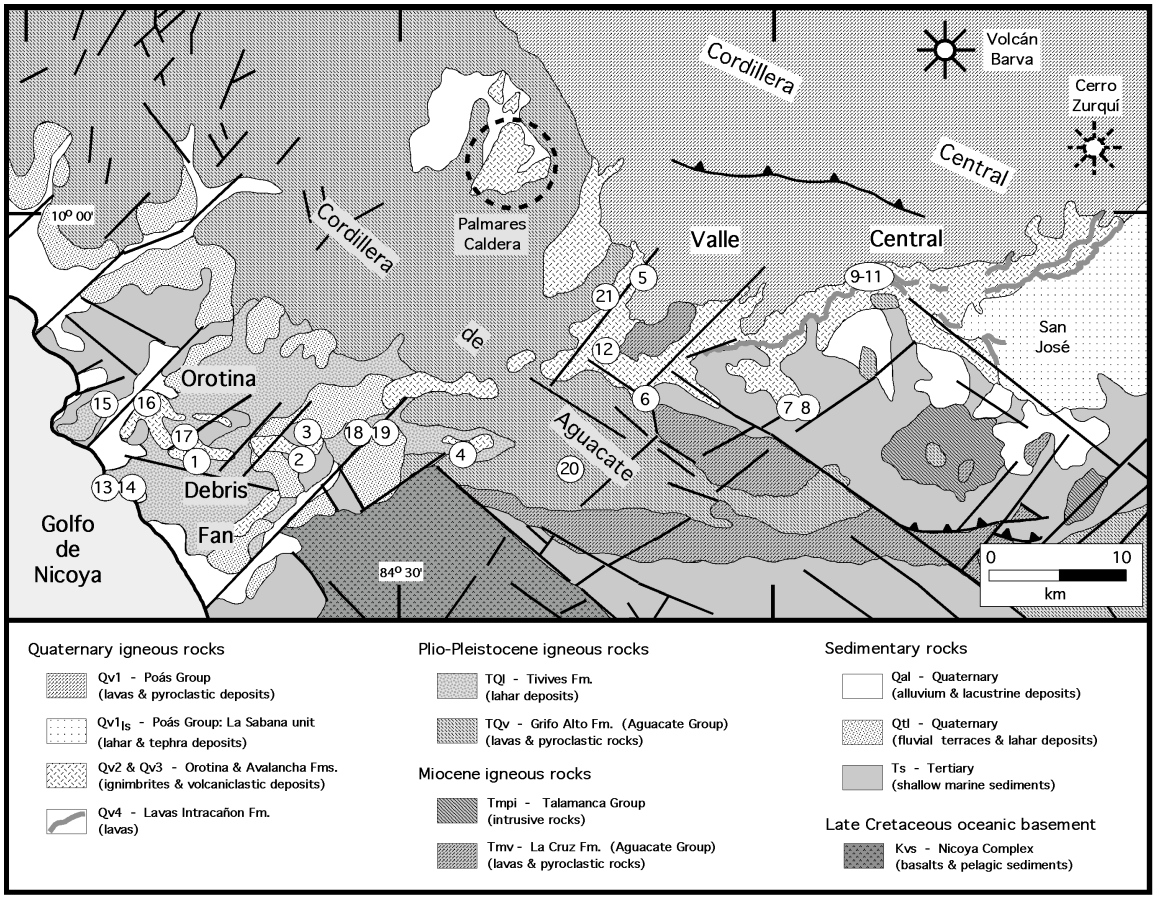

Figure 4. Geologic map of the volcanic arc of central Costa Rica (from Marshall, 2000). Numbered cirlces indicate 40Ar/39Ar dated sample locations (see Table 1 for sample data). Quaternary volcanoes indicated by radial spokes; solid lines, active; dashed lines, inactive. Extinct Quaternary caldera outlined by dashed circle. Solid lines mark faults of the Central Costa Rica Deformed Belt (Marshall et al., 2000). Geologic data are modified from Madrigal (1970), Bergoeing et al. (1980), Ministerio de Industria, Energia y Minas (1982), Denyer and Arias (1991), Denyer et al. (1993), Protti and Schwartz (1994) and Marshall (2000).

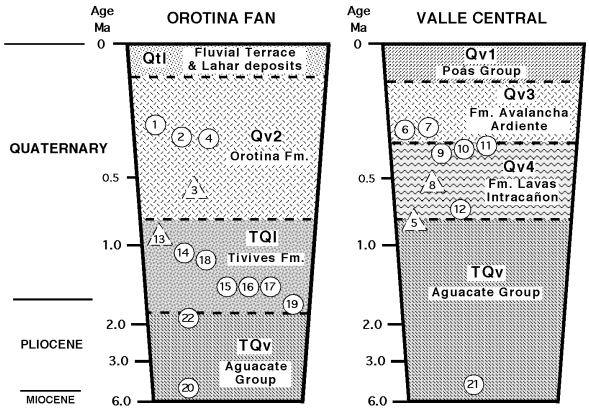

Figure 5. Comparative stratigraphic columns for the Orotina debris fan and Valle Central showing age distribution of 40Ar/39Ar samples (from Marshall, 2000). Circles indicate well-constrained sample ages, and triangles show maximum ages. Sample numbers refer to Fig. 4 and Table 1. Background symbols correspond with geologic map in Fig. 4.

Table 1. 40Ar/39Ar Age Results

Sample Number	Field ID Number	Rock Type (Material Dated)	Location	Lat.	Long.	Plateau Age	Isochron Age	MSWD
Formación Orotina (Qv2)								
1	CR94-32	welded tuff (plagioclase)	Cerro Túnel, Ceiba de Orotina	9° 53'	84° 38'	**326 ±18 ka**	(342 ± 44 ka)	3.56
2	CR93-13	welded tuff (plagioclase)	Quebrada Santa Rita, Costanera highway	9° 52'	84° 35'	384 ± 18 ka	**352 ± 40 ka**	0.89
3	CR94-21	ash (biotite)	Jacó-Orotina junction, Costanera highway	9° 53'	84° 35'	----------	(664 ± 109 ka)	3.89
4	CR95-26	welded tuff (plagioclase)	San Pedro, Turrubares	9° 52'	84° 28'	391 ± 13 ka	**373 ± 19 ka**	0.69
Formación Avalancha Ardiente (Qv3)								
5	CR93-25	tuff (plagioclase)	Tajo La Aduana, La Garita	10° 00'	84° 20'	(938 ± 55 ka)	(925 ± 86 ka)	2.60
6	CR96-1	welded tuff (plagioclase)	Río Picagres, Picagres de Mora	9° 55'	84° 20'	(328 ± 15 ka)	**331 ± 23 ka**	2.08
7	CR96-2	welded tuff (biotite)	Quebrada Honda, Ciudad Colón	9° 54'	84° 15'	**320 ± 10 ka**	(313 ± 15 ka)	3.25
8	CR93-9	ash (biotite)	Quebrada Honda, Ciudad Colón	9° 54'	84° 15'	(527 ± 24 ka)	(597 ± 54 ka)	2.58
9	CR94-35	welded tuff (plagioclase)	Tajo Pedregal, San Antonio de Belén	9° 58'	84° 11'	387 ± 17 ka	**390 ± 17 ka**	0.08
Formación Lavas Intracañon (Qv4)								
10	CR94-34	andesite lava (groundmass)	Tajo Pedregal, San Antonio de Belén	9° 58'	84° 11'	375 ± 22 ka	**371 ± 49 ka**	1.97
11	CR94-33	andesite lava (groundmass)	Tajo Pedregal, San Antonio de Belén	9° 58'	84° 11'	341 ± 6 ka	**337 ± 7 ka**	1.00
12	CR95-6	andesite lava (groundmass)	Cebadilla, Turrucares	9° 56'	84° 21'	775 ± 10 ka	**758 ± 16 ka**	1.16
Formación Tivives (Qvl)								
13	CR94-7a	lahar (biotite)	Bajamar, Tivives	9° 50'	84° 41'	(908 ± 20 ka)	(909 ± 53 ka)	4.35
14	CR94-7b	lahar (plagioclase)	Bajamar, Tivives	9° 50'	84° 41'	1.14 ±0.07 Ma	**1.10 ± 0.07 Ma**	1.01
15	CR93-12	lahar (biotite)	Alto de las Mesas, Tivives	9° 55'	84° 42'	----------	**1.42 ± 0.13 Ma**	2.15
16	CR94-9	lahar (plagioclase)	Río Jesús María Costanera highway	9° 55'	84° 40'	1.53 ± 0.04 Ma	**1.45 ± 0.05 Ma**	0.17
17	CR94-38	welded tuff (biotite)	Cerro Tamarindo, Ceiba de Orotina	9° 53'	84° 38'	(1.91 ± 0.03 Ma)	**1.45 ± 0.07 Ma**	1.27
18	CR94-18	pumice/sand (plagioclase)	Puente Agres, Orotina	9° 53'	84° 32'	(1.26 ± 0.13 Ma)	**1.12 ± 0.13 Ma**	2.36
19	CR94-16	lahar (plagioclase)	Puente Agres, Orotina	9° 53'	84° 32'	(2.39 ± 0.03 Ma)	**1.66 ± 0.16 Ma**	0.92
Grupo Aguacate: Formación Grifo Alto (TQga)								
20	CR94-13	andesite lava (groundmass)	Cruz de Guatuso, Puriscal	9° 51'	84° 23'	**5.01 ± 0.11 Ma**	(5.02 ± 0.39 Ma)	7.76
21	CR93-24	trachyte lava (plagioclase)	Tajo La Aduana, La Garita	9° 59'	84° 21'	5.55 ± 0.05 Ma	**5.52 ± 0.08 Ma**	0.51
Grupo Aguacate: undifferentiated								
22	CR97-1	andesite lava (groundmass)	Cerro Coronacíon Cañas-Tilarán highway	10° 28'	85° 04'	2.08 ± 0.26 Ma	**1.90 ± 0.05 Ma**	1.71

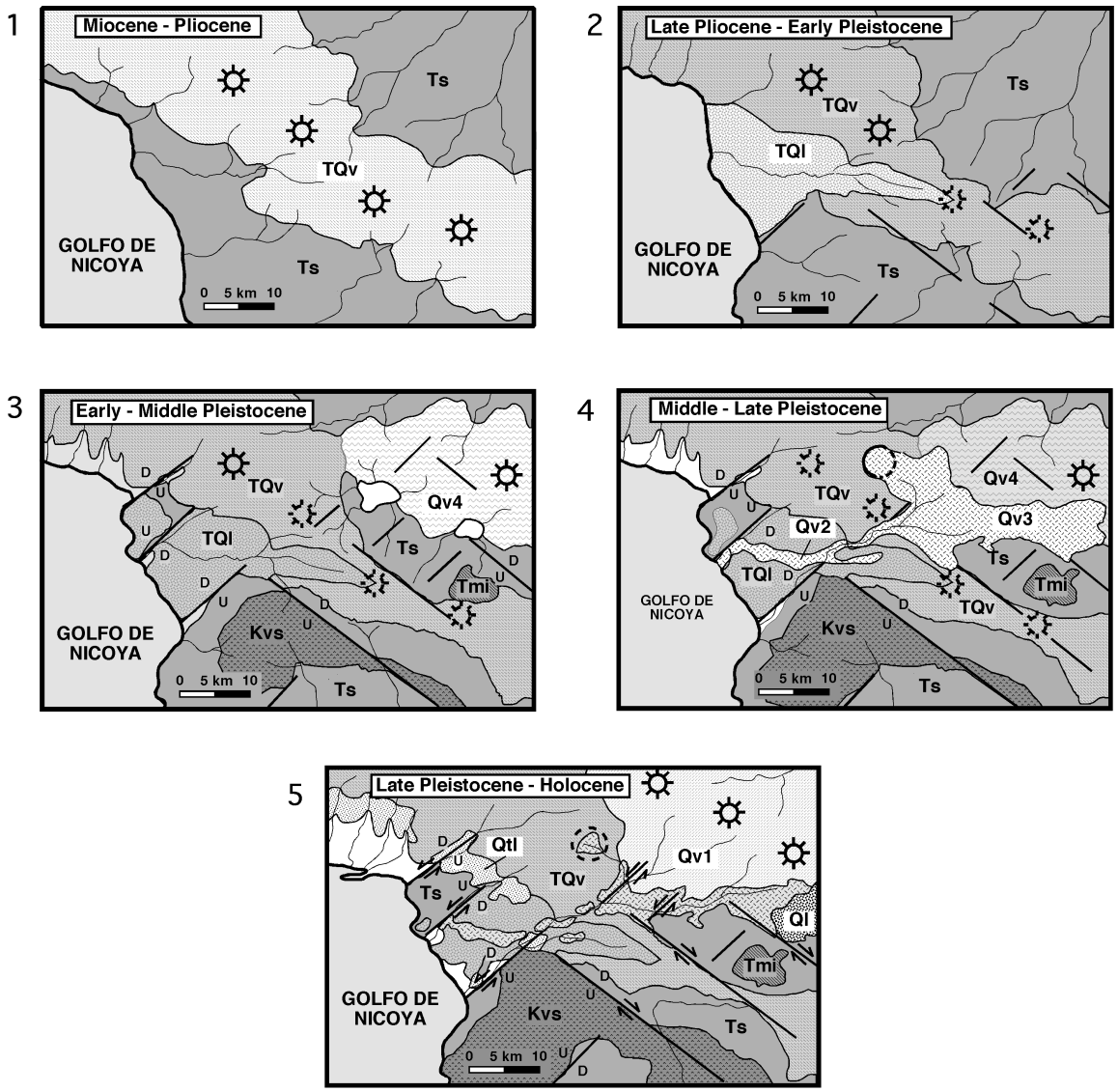

Figure 6. Five stage geologic model for late Cenozoic landscape evolution of the central Costa Rican volcanic arc (from Marshall, 2000). White background in each map indicates units deposited during that particular time stage. (See Fig. 4 for explanation of geologic symbols.) The late Neogene onset of flat subduction led to northeastward retreat of the volcanic arc, formation of the Valle Central, reorganization of drainage divides, deposition of the Orotina debris fan on the Pacific slope, and diffuse faulting across the arc along the Central Costa Rica deformed belt.

DAY 1 (afternoon)

Thursday, 5 July 2001

The Península de Nicoya: Caribbean basement, subduction erosion, & seamount driven uplift

Road Log (Day 1, afternoon):

We will board a ferry at Puntarenas and cross the Golfo de Nicoya to the southeastern coast of the Península de Nicoya (Fig. 7). This part of the coastal fore arc (Fig. 3, site 11) lies directly inboard of the subducting rough-smooth boundary on the Cocos plate. The ferry ride will provide an excellent view of the morphology and structure of the central Pacific coast and volcanic arc.

Looking back toward the mainland, you will see variations in topographic relief along the coastline that correspond with differentially uplifted fore arc fault blocks. The Esparza block (moderate uplift) stands out clearly as the flat topped mesa southeast of Puntarenas. The Orotina block (low uplift) corresponds with the low relief segment of coast stretching further to the southeast. To the far right, the peak of Cerro Turrubares towers above the prominent headland of the Herradura block (high uplift). Inland of these coastal blocks, the eroding remnants of the Aguacate volcanic range stretch along the horizon. Just visible above the crest of the Aguacate divide are several peaks of active volcanoes in the Cordillera Central.

After arriving at the port of Paquera on the Península de Nicoya, we will drive a short distance around Bahía Ballena to the Tango Mar beach resort where we will spend the night. After check-in, we will explore coastal outcrops along the Tango Mar beach.

Geologic Overview (Day 1, afternoon):

Península de Nicoya: The base of slope sediment unconformity

A prominent feature in offshore seismic reflection profiles (Fig. 7) of the fore arc is a rough, irregular reflector that represents the base of low-velocity slope sediments ("BOSS reflector") overlying a higher-velocity wedge that extends out to the lower slope (Stoffa et al., 1991; Shipley et al., 1992; McIntosh et al., 1993; Hinz et al., 1996). The high-velocity wedge has been explained alternatively as either a package of accreted Tertiary sediments (Shipley et al., 1992) or as Cretaceous-early Tertiary oceanic basement rocks (Nicoya Complex) similar to those observed in onshore exposures (von Huene and Flüh, 1994; Donnelly, 1994).

Leg 170 of the Ocean Drilling Program drilled through the upper-slope sediments offshore of the Península de Nicoya (site 1042) and encountered a breccia consisting of oceanic basalt fragments within a Miocene matrix (Kimura et al., 1997; Vannuchi et al., 2000). This suggests that localized exposures of oceanic basement rocks along coastal peninsulas and headlands may

represent sections of a continuous fore-arc basement uplifted along faults that offset the rough reflector (Fig. 7; Fisher et al., 1998). These basement exposures coincide with the highest Quaternary uplift rates in the fore arc, such as those recorded near the southern tip of the Península de Nicoya (Marshall and Anderson, 1995; Gardner et al, 2001).

Basement rocks exposed on the Península de Nicoya (Fig. 7) consist of the Cretaceous-early Tertiary Nicoya Complex, an intensely deformed oceanic sequence of pillow basalts, mafic intrusive rocks, and pelagic sediments (de Boer, 1979; Kuijpers, 1980; Lundberg, 1982; Baumgartner et al., 1984; Bourgois et al., 1984; Donnelly, 1994; Di Marco et al., 1995; Sinton et al., 1997). Along the margins of the peninsula, a sequence of upper Cretaceous to Quaternary marine sediments (Garza and Malpaís supergroups) drapes unconformably across the Nicoya Complex basement. These sediments include Cretaceous-Paleocene turbidites, Eocene deep water carbonates, Miocene shelf clastics and a shallowing upward sequence of Plio-Pleistocene shelf sandstones and conglomerates (Lundberg, 1982; Baumgartner et al., 1984).

The youngest sedimentary rocks exposed on the peninsula (Fig. 7) consist of the Plio-Pleistocene shallow marine sandstones and conglomerates of the Montezuma Fm. (Dengo, 1962; Lundberg, 1982 and 1991; Chinchilla, 1983; Mora, 1985). This unit overlies the Nicoya Complex along a highly irregular unconformity that probably represents an erosional surface on prior emergent topography. This prominent unconformity suggests that Tertiary emergence may have been interrupted by a period of subsidence allowing for deposition of the shallow water Montezuma Fm. (Marshall, 1991).

The presence of nearshore bioclastic material in contact with oceanic basement fragments at a depth of 3900 m at drilling site 1042 is suggestive of an episode of subsidence that may reflect extensive outer arc subduction erosion (Vannucchi et al., 2000). A local return to uplift near Cabo Blanco, beginning in the middle Pleistocene, led to emergence of the Montezuma Fm. and erosion of the Cobano marine terrace during sea level high stands of the late Pleistocene. This rapid uplift may be the result of the subduction of the Fisher seamount chain beneath Cabo Blanco (Marshall and Anderson, 1995; Gardner et al., 2001).

Day 1 Field Trip Stops:

Stop 1. Tango Mar beach (Playa Quizales)

Coastal cliffs at the Tango Mar beach resort expose of the unconformity between the shallow water sands of the Plio-Pleistocene Montezuma Fm. and the underlying late Cretaceous-early Tertiary oceanic basement rocks of the Nicoya Complex. Coastal exposures of neritic sediments overlying the mafic and pelagic basement rocks have been correlated with the base of slope sediment horizon (BOSS reflector) observed in offshore seismic profiles (Vannucchi et al., 2000).

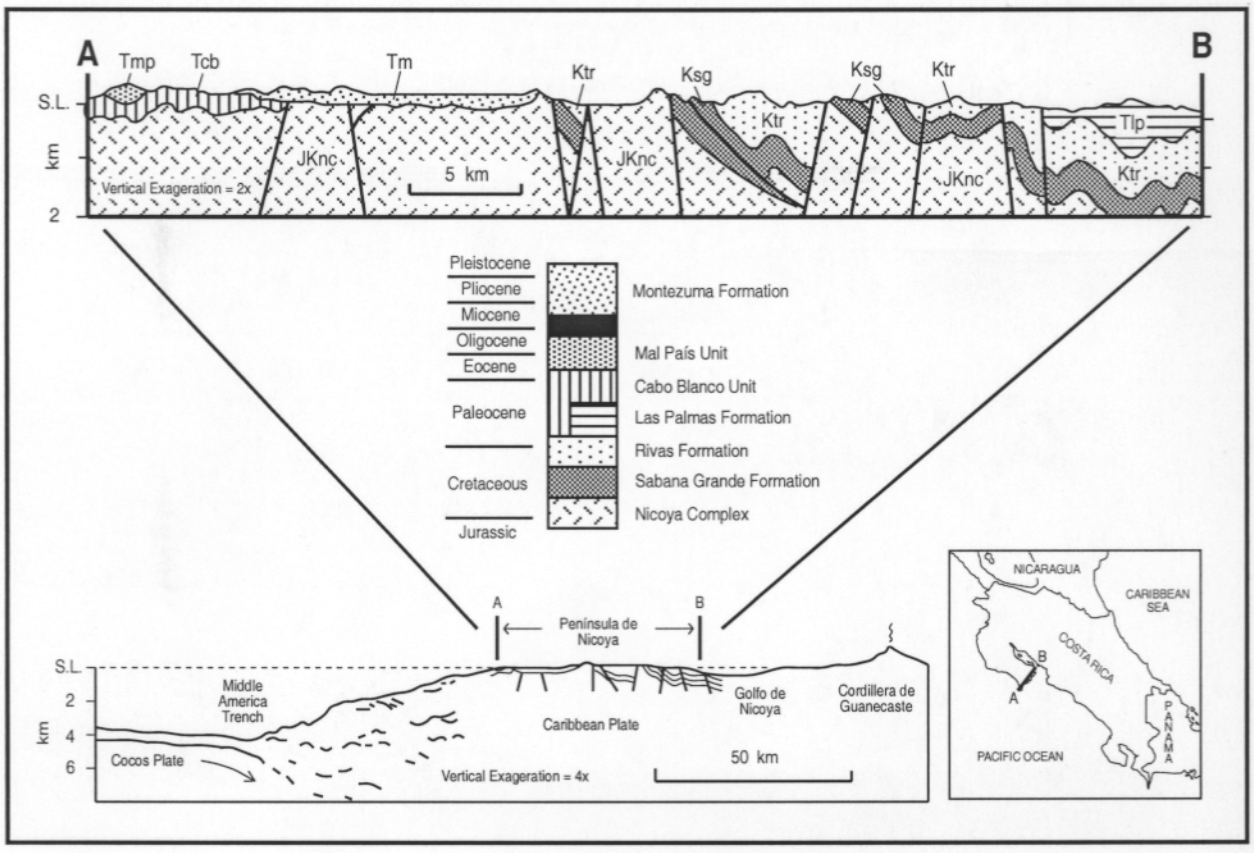

Figure 7. Geologic cross section perpendicular to the Middle America Trench along the southeast coast of the Península de Nicoya (modified from Lundberg, 1991).

DAY 2

Friday, 6 July 2001

Seamount subduction and Quaternary uplift at Cabo Blanco, Península de Nicoya

Road Log (Day 2):

During this morning's portion of the field trip, we will visit a flight of Quaternary marine terraces (Cobano and Cabuya surfaces) near Cabo Blanco (Fig. 3, site 11) and observe evidence for uplift and rotation of the southern tip of the Península de Nicoya (Fig. 8) caused by seamount subduction. As we drive from the Tango Mar resort to Cabo Blanco, we will cross the broad dissected mesa of the late Pleistocene Cobano terrace. This surface is bounded by the interior mountain range on the north, the Cabo Blanco highland to the south, and abandoned sea cliffs along shorelines to the southwest and southeast (Fig. 8). As we approach the southeastern shoreline, the road will descend abruptly down the Cobano cliff to the low-lying Holocene Cabuya terrace at the coastal town of Montezuma. We will then follow the coastline southward along the narrow Holocene terrace to the village of Cabuya near Cabo Blanco.

Geologic Overview (Day 2):

Quaternary marine terraces of the southern Península de Nicoya

The southern tip of the Península de Nicoya is located ~60 km inboard of the rough-smooth boundary and the subducting Fisher seamount chain on the Cocos plate (Fig. 3, site 11). Two prominent uplifted Quaternary marine terraces occur in this area near Cabo Blanco (Fig. 8). With two orthogonal coastlines, oriented parallel and perpendicular to the margin, this site provides an ideal location to evaluate fore arc block uplift using marine terraces. The upper terrace, referred to as the Cobano surface (Hare and Gardner, 1985; Mora, 1985), consists of an extensive (~120 km^2) deeply incised coastal mesa lying between the interior mountains and the abandoned Cobano sea-cliff. This surface shows a gentle northward dip, descending from over 200 m near Cabo Blanco to less than 80 m inland from the town of Cobano (Fig. 8). This terrace is cut across the Plio-Pleistocene shallow marine sediments of the Montezuma Fm., Paleogene turbidites of the Cabo Blanco Fm., and the late Cretaceous oceanic basalts of the Nicoya Complex. Uplift, beginning in the mid to late Pleistocene, led to emergence of the peninsula's southern tip and erosion of the Cobano surface during sea level highstands of the late Pleistocene (Mora, 1985; Marshall, 1991; Marshall and Anderson, 1995).

The lower terrace, referred to as the Cabuya surface (Marshall, 1991) consists of two adjacent, relatively narrow (< 1 km), low-lying (< 20 m elevation) wavecut platforms located along the

seaward edge of the Cobano terrace between the abandoned Cobano sea-cliff and the modern shoreline (Fig. 8; Marshall, 1991; Marshall and Anderson, 1995; Gardner et al., 2001). Both the lower (I) and upper (II) Cabuya platforms are cut across the basalts of the Nicoya Complex and the folded turbidites of the Cretaceous-Eocene Cabo Blanco Fm. These platforms are covered with up to 2 m of fossiliferous, intertidal sands, gravels, and beach rock (Calvo, 1983; Chinchilla, 1983). Radiocarbon dating of 35 samples yielded late Holocene ages ranging between 0.3 - 7.4 ka (Marshall, 1991; Marshall and Anderson, 1995; Gardner et al., 2001).

Uplift rates and block rotation

Inner edge elevations for the wavecut Cabuya platforms descend systematically along both coastlines away from Cabo Blanco (0 km, Fig. 8). At ~20 km from Cabo Blanco along both coastlines, the platforms converge to approximately modern mean sea level (Fig. 9a). Uplift rates decrease linearly from a maximum of ~6.0 m/ky near Cabo Blanco, to <1.0 m/ky along the 20 km length of both the margin-perpendicular and margin-parallel coastlines (Fig. 9b; Marshall and Anderson, 1995; Gardner et al., 2001). The 400km^2 tip of the peninsula is rotating northward as a discrete block with an angular rotation rate of 0.02^o/ky about an axis with an azimuth of 80^o. This distribution of uplift is consistent with the elevation and tilt of the late Pleistocene Cobano terrace with uplift beginning at <~250 ka.

Deformation by seamount subduction

The observed uplift and block rotation at the southern tip of the Península de Nicoya may be the result of seamount subduction along the projected trend of the rough-smooth boundary and the Fisher seamount chain (Marshall and Anderson, 1995; Gardner et al., 2001). The Caribbean plate margin offshore is extensively scalloped (Fig. 3) with headwall scarps and subsidence features within 20 km of the Península de Nicoya coastline (Dominquez, 1998 and 2000; von Huene et al., 1995 and 2000). The Benioff zone occurs at ~20 km depth beneath the tip of the peninsula and the 1990 Cobano subduction earthquake (Mw =7.0, depth = 20km) was located just offshore of Bahía Ballena (Fig 8). The arcuate distribution of aftershocks (Fig. 12) suggests that the rupture may be related to seamount subduction along the trend of the rough-smooth boundary (Protti et al., 1995).

The wavecut treads of the Cabuya terrace exhibit multiple, small (<1 m), laterally discontinuous steps that may record episodic, co-seismic uplift (Anderson et al., 1989; Marshall, 1991; Marshall and Anderson, 1995; Gardner et al., 2001). These steps are not, however, resolvable with radiocarbon dating. They probably indicate short time step (<100 yr), nonlinear, co-seismic uplift events which are averaged by the long-term (1000's yrs) linear uplift rates.

Seamount subduction beneath Cabo Blanco would produce the observed rotation of the Holocene Cabuya terrace away the tip of the peninsula along both the margin-parallel and margin-perpendicular coastlines. If this rotation is limited to approximately the last 250 ka, as constrained by emergence of the late Pleistocene Cobano terrace, then a seamount subducting at the modern

convergence rate of ~9 cm/yr would have migrated < 20 km along the convergence vector. This distance is consistent with the ~400 km^2 area of the uplifting block and the dimensions of larger seamounts in the Fisher seamount chain (Fig. 3).

Seamounts may be underplating onto the Caribbean plate or may remain attached to the Cocos plate and continue subducting. Underplating would produce permanent and cumulate vertical displacement in the overriding plate as the line of seamounts subducts. If seamounts remain attached to the Cocos plate, then subsidence may occur after passage as observed along the margin slope offshore (von Huene et al., 1995 and 2000; Dominquez et al., 1998 and 2000).

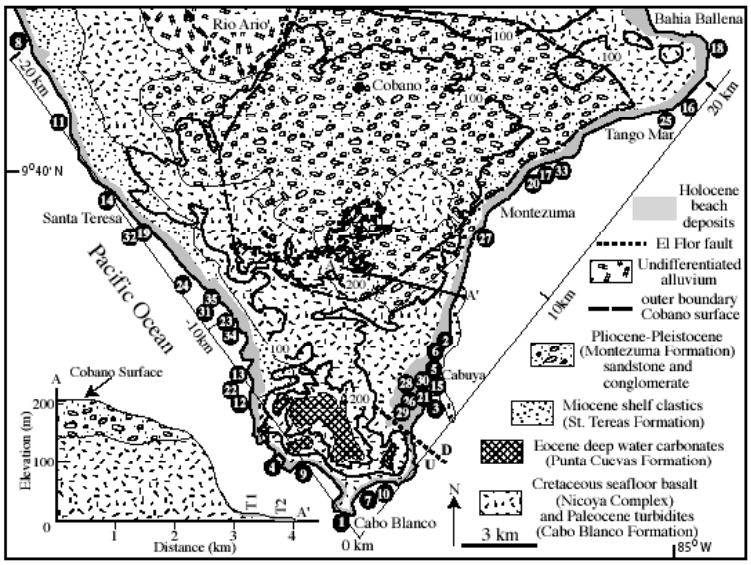

Figure 8. Geologic map of the southern tip of the Península de Nicoya (from Gardner et al., 2001). Geology after Baumgarter et al. (1984), Mora and Baumgarter (1985), Mora (1985), and Marshall and Anderson (1995). Heavy line along the coast marks approximate mean sea level. Numbers mark radiocarbon sample locations. Lines along Pacific and Gulf coasts (distance in kms, with O km at Cabo Blanco) coincide with x-axis in Fig. 9.

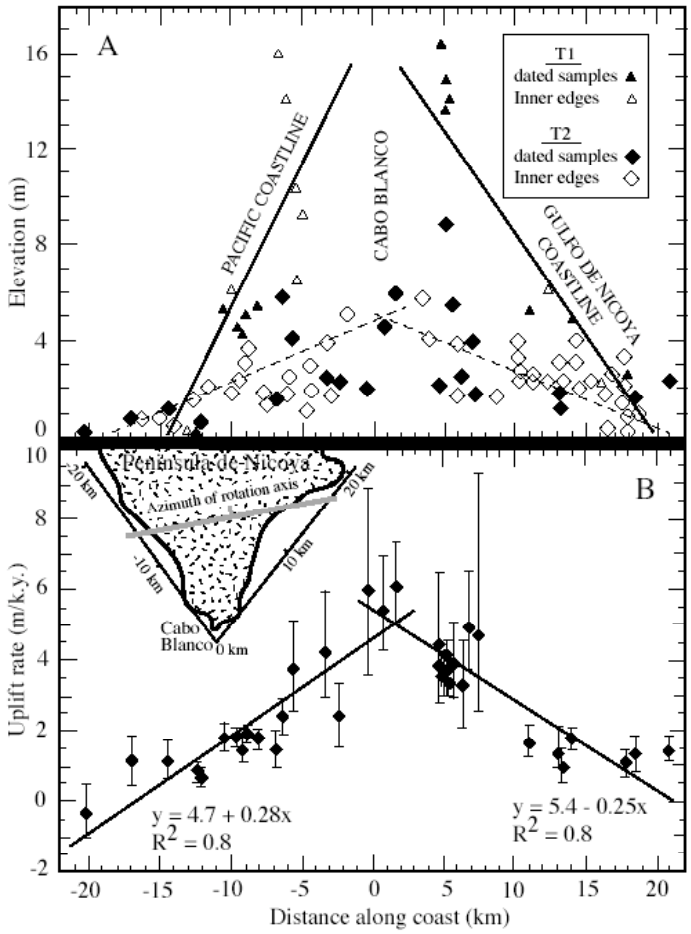

Figure 9. a) Elevation vs distance plot (from Gardner et al., 2001) for dated samples and undated terrace inner edges (paleo-high tide line) showing distinct elevation trends for the two Cabuya platforms. X-axis measures distance along both coastlines, with axis location shown on Fig. 8 and in inset of Fig. 9b. b) Calculated uplift rates with error bars for all dated samples. Linear best-fit regression lines (equations at bottom) illustrate the significant decrease in uplift rates away from the peninsula' s tip at Cabo Blanco. Thick grey line in inset indicates azimuth direction for block rotation axis with tick on downdip side.

Day 2 Field Trip Stops:

Stop 1. Playa Cabuya intertidal platform - Marine terrace formation

The Holocene Cabuya terrace (Marshall, 1991) consists of two parrallel, low-lying (0-20 m elev.) wavecut platforms located between the ocean and the abandoned sea cliffs rising up to the late Pleistocene Cobano terrace (Fig. 10). Near Montezuma, the Cabuya surface is relatively narrow (< 200 m) with a rugged, rocky shoreline cut in resistant basalts of the Nicoya Complex. At Cabuya, however, the surface widens (~1 km) into a gently sloping coastal terrace formed across the folded turbidites of the Paleogene Cabo Blanco Fm. In contrast to the rocky shoreline formed in the basalts, wave action at Cabuya has abraded the less resistant sediments into a broad, gently dipping intertidal platform. At low tide, the ocean retreats as much as 500 m (tidal range = ~3 m), exposing a large expanse of the intertidal platform (Fig. 10). This wavecut surface represents a superb modern analog for Quaternary marine terrace formation during sea level high stands.

A small flat-topped island (Isla Cabuya), at the seaward margin of the active intertidal platform (Fig. 10) preserves a remnant of a higher wavecut platform (~3-4 m elev.). At high tide, Isla Cabuya is surrounded by water, but as falling tide exposes the intertidal platform, the island becomes connected to the mainland. The island's surface is covered by unconsolidated fossiliferous beach sands with a radiocarbon age of 490 ± 60 yr. B.P. (Marshall, 1991). The Isla Cabuya platform may reflect one or more coseismic uplift events related to seamount subduction beneath this area (Anderson et al., 1989; Marshall, 1991; Marshall and Anderson, 1995).

Stop 2. Cabuya Terrace - Late Holocene uplift and coastal emergence

Walking inland from the beach, we will traverse the width of the uplifted Cabuya surface from the active shoreline to the abandoned sea cliff at the edge of the Pleistocene Cobano terrace (Fig. 10). Along this transect, the wavecut surface on the underlying bedrock is covered by an unconsolidated blanket (1-3 m thick) of fossiliferous intertidal sands and gravels. A 3-5 m high scarp divides the surface into the lower (I) and upper (II) Cabuya platforms. Topographic profiles (Fig. 11) surveyed across this transect show the locations of radiocarbon dated samples used to calculate uplift rates (Marshall, 1991).

Emergence of the Cabuya surface requires uplift rates that exceed the rate of late Holocene sea level rise. The rapid post-glacial rise in global sea level began to slow dramatically near 7.0 ka approaching the modern high stand (Fairbanks, 1989; Chappell and Polach, 1991). After 7.0 ka, the rate of sea level rise decreased from >5 m/ky to <1.5 m/ky. Calculated uplift rates at Cabuya (~4.0 m/ky) are less than the rate of sea level rise prior to this time and greater than the rate of sea level rise afterwards. Therefore, the sudden slowing of sea level rise around 7.0 ka initiated a local marine regression, emergence of the uplifting Cabuya terrace, and progressive abandonment of shore deposits stretching across the terrace surface (Figs. 10 and 11; Marshall 1991; Marshall and Anderson, 1995). Radiocarbon ages for these deposits span the late Holocene ranging from a

maximum of 7.4 ky near the base of the Cobano cliff to 0.3 ky near the shoreline. The abandoned Cobano seacliff marks the shoreline at the beginning of emergence, when the rate of sea level rise was equal to the rate of rock uplift.

Stop 3. Cobano Terrace - Late Pleistocene wavecut surface

Climbing up the abandoned sea cliff at the back edge of the Cabuya surface, we will reach the broad upland surface of the Cobano terrace (Fig. 10). From this vantage point, we will have a superb view of the Holocene Cabuya terrace, the Cabo Blanco headland, and the mainland coast across the Golfo de Nicoya. Looking inland, you can see the concordant hilltops that define the highly dissected Cobano surface (Figs. 8 and 10). This late Pleistocene marine erosional surface is cut across sediments of the Paleogene Cabo Blanco Fm., the Plio-Pleistocene Montezuma Fm., and late Cretaceous oceanic basalts of the Nicoya Complex (Mora, 1985; Hare and Gardner, 1985; Marshall and Anderson, 1995). The Cobano surface probably represents a composite marine terrace encompassing several wavecut surfaces formed during the multiple sea level high stands of the late Pleistocene (Marshall, 2000). Together, the Cobano and Cabuya surfaces record rapid uplift and arcward tilting generated by seamount subduction beneath Cabo Blanco (Marshall and Anderson, 1995; Gardner et al., 2001).

Stop 4. Cabo Blanco coastal bluffs - Quaternary uplift and the earthquake cycle

Several aspects of the Cabuya terrace suggest that Holocene uplift near Cabo Blanco may reflect the net accumulation of episodic seismic-cycle uplift (Anderson et al., 1989; Marshall, 1991; Marshall and Anderson, 1995; Gardner et al., 2001): 1) multiple, widely-spaced paleo-beach ridges mark apparent jumps in shoreline position; 2) similarly, stream bank exposures reveal occasional small steps (~1m) in the wavecut tread; 3) delicate coral debris mantling the remnant platform of Isla Cabuya suggests rapid uplift through the wave base; and 4) stratigraphy within the 5 m tall beach cliff adjacent to the Cabo Blanco Natural Rerserve headquarters reveals multiple paleosols separating intertidal and fluvial sediments with a spacing of 1-2 m.

Popular legends and historical records describe the recurrence of severe earthquakes on the Península de Nicoya (González-Víquez, 1910; Pittier, 1959; Marshall, 1991). For example, the legend of Cerro de las Cruces tells of a monstrous serpent that causes earthquakes while trying to escape from inside a mountain near the heart of the peninsula (Pittier, 1959; Zeledon, 1989). Historical documents from the colonial town of Nicoya record periodic repairs made to the parochial church in the wake of large earthquakes.

During the 20th century, modern seismographic networks recorded at least five large subduction earthquakes ($M \geq 7.0$) in the vicinity of the Península de Nicoya (Fig. 12; Güendel, 1986; Protti et al., 1995). Two of these events (1939, $M_S = 7.1$; 1990, $M_W = 7.0$) occurred near the entrance to the Golfo de Nicoya and may reflect the rupture of seamount related asperities along the

trend of the rough-smooth boundary (Protti et al., 1995). Earthquakes located in this area could potentially generate coastal uplift near Cabo Blanco.

The largest historically recorded earthquake along the Costa Rica coast (5 October 1950, M = 7.7) and a later smaller event (1978, M_S = 7.0) were centered directly beneath the peninsula (Güendel, 1986). With a rapid convergence rate of 9 cm/yr along this segment of the trench (DeMets and others, 1990), it is unlikely that the smaller 1978 earthquake released all of the strain accumulated since the much larger 1950 event (Güendel, 1986). Nishenko (1989) gives a 93% probability of a M 7.4 earthquake on the Península de Nicoya before the year 2009, listing it as fourth among the top seismic gaps in the circum-Pacific region.

Substantial coastal uplift associated with the 1950 Nicoya earthquake was documented through interviews with local residents (Marshall, 1991; Marshall and Anderson, 1995). Eyewitnesses indicate that coseismic uplift of at least 1m affected the coastline between Puerto Carrillo and Nosara, and that a significant fraction of this uplift has been recovered over the past five decades by gradual subsidence. Ongoing subsidence is manifested along much of the peninsula's coastline by rapid coastal erosion and the submergence of historical structures (Marshall, 1991).

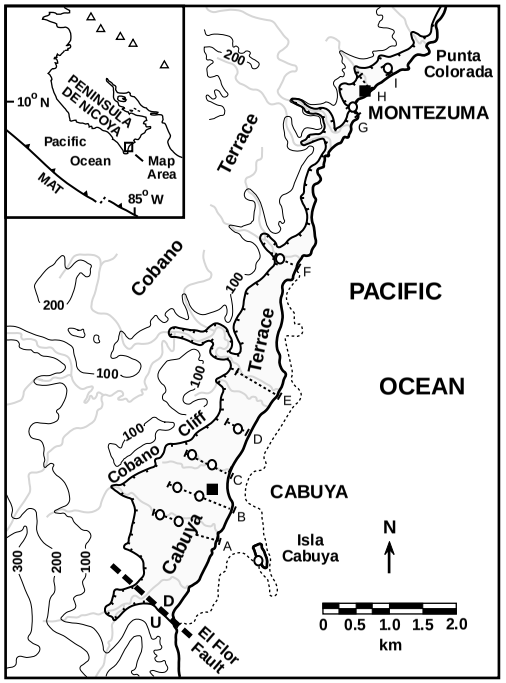

Figure 10. Map of the coastline between Montezuma and Cabuya showing the Holocene Cabuya surface along the seaward edge of the late Pleistocene Cobano terrace (from Marshall, 1991). Letters with dashed lines mark the location of nine topographic profile lines (e.g., Fig. 11) where radiocarbon samples were collected (circles). The Cabuya surface lies between the modern shoreline (heavy solid line) and the abandoned Cobano sea cliff (heavy stippled line). Dashed line offshore marks the seaward limit of the extensive intertidal platform at Playa Cabuya..

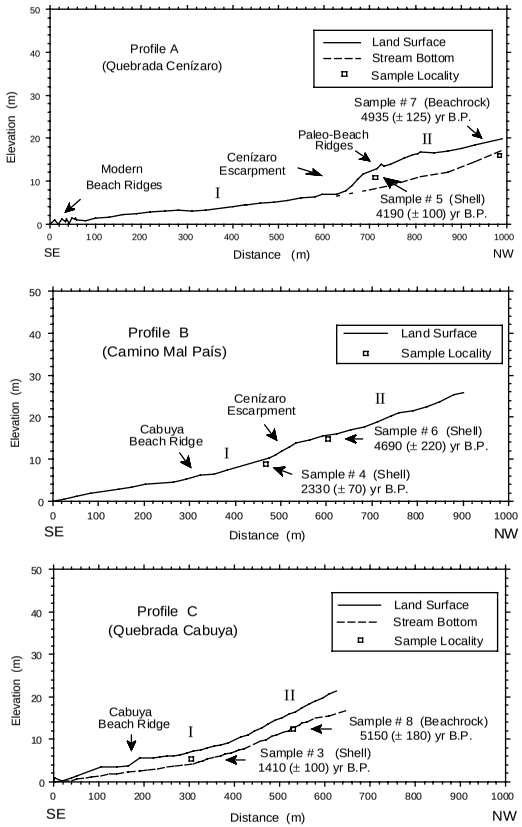

Figure 11. Examples of topographic profile lines across the Cabuya surface showing radiocarbon sample locations (from Marshall, 1991). See Fig. 10 for locations. Distance and elevation are from the strandline marking highest high tide (approx. 1.5 m above MSL) along the modern shoreline.

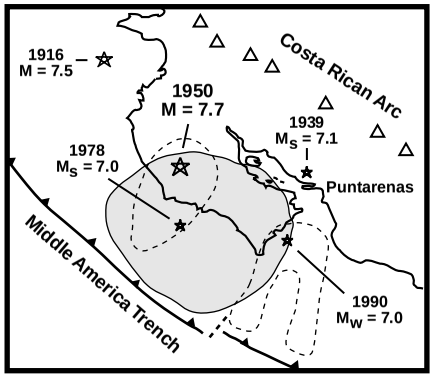

Figure 12. Locations of 5 recent large subduction earthquakes (M ≥ 7.0) centered near the Península de Nicoya (from Marshall, 1991). Stars represent epicenters. Shaded area within solid line is aftershock area for the 1950 event. Dashed lines enclose aftershock areas for the 1978 and 1990 events. Data from Güendel (1986) and Protti (1991 and 1994).

DAY 3:

Saturday, 7 July 2001

Quaternary geology and tectonics of the Orotina and Esparza blocks

Road Log (Day 3):

During today's segment of the field trip, we will explore the Quaternary geology, geomorphology, and structure of the Orotina and Esparza blocks (Fig. 13) directly onshore of the subducting rough-smooth boundary (Fig. 3, sites 3-5). We will drive northward from Villa Lapas to the Río Tárcoles (Fig. 13), where we will observe a flight of Quaternary fluvial terraces. This major river is the principal drainage of the Valle Central and a prime habitat for the endangered American crocodile. The river flows along the NE striking Tárcoles fault, which accomodates rapid uplift of the Herradura block relative to the low-lying Orotina block.

We will then continue across the Orotina block to look at Quaternary volcanic stratigraphy at a coastal outcrop near Playa Bajamar and a quarry near the Río Jesús María. Mapping and $^{40}Ar/^{39}Ar$ dating of this sequence demonstrates a link between the Orotina debris fan at the coast and the volcanic stratigraphy of the Valle Central (Figs. 4 and 5; Table 1).

We will continue to the Jesús María fault scarp betweent the Orotina and Esparza blocks (Fig. 13). There, we will examine offset strata and mesoscale faults that record transtensional kinematics across the major block bounding faults. Driving up to the top of Alto de las Mesas on the Esparza block, we will then enjoy an excellent view across the Orotina debris fan and the differentially uplifted fault blocks of the coastal fore arc region. From there, we will proceed to the village of Mata de Limón for lunch along a coastal mangrove estuary.

In the afternoon, we will drive to the Río Barranca along the NW edge of the Esparza block (Fig. 13) to view a flight of Quaternary fluvial terraces that have been offset along the Barranca fault. Correlation of these terraces with those studied along other coastal rivers provides a means for evaluating uplift along the entire Costa Rican Pacific margin. We will then return across the Orotina debris fan to Villa Lapas for swimming and a sunset happy hour.

Geologic Overview (Day 3):

Orotina debris fan

The Pacific coastline between Puntarenas (Fig. 3, near site 2) and the Herradura headland (Fig. 3, "H") consists of a relatively low-relief (<250 m) coastal plain (750 km^2) along the foot of the extinct Aguacate volcanic range. This region includes the lower drainage basins of the ríos Barranca, Jesús María, and Tárcoles (Fig. 3, sites 3-5) which flow southwestward into the Golfo de Nicoya. These rivers follow fault-controlled valleys (Fig. 13) incised within a large alluvial fan referred to as the Orotina debris fan (Marshall, 2000).

The stratigraphic framework of the Orotina debris fan consists of a >100 m thick package of Quaternary volcanic debris flows, pyroclastic deposits, volcaniclastic sands, and fluvial gravels (Fig. 13). Early Quaternary explosive volcanism in the Aguacate range generated major lahars (Tivives Fm.; Madrigal, 1970) which descended across the 25 km wide coastal plain between the ríos Tárcoles and Barranca. Pleistocene retreat of the volcanic front from the Cordillera Aguacate to the Cordillera Central led to formation of the Valle Central basin between the two ranges (Fig. 6). This new basin rapidly filled with lacustrine sediments, lavas, pyroclastic flows, and lahars.

Headward erosion across the Aguacate drainage divide led to rapid stream capture within the Valle Central and deep incision of the modern drainage system funneling toward the Tárcoles gorge (Marshall, 2000). This shift in the location of the Pacific-Caribbean drainage divide opened a pathway for pyroclastic flows (Orotina Fm.; Madrigal, 1970) to spill over onto the Orotina debris fan at the Pacific coast (Fig. 13). Meandering paleo-channels of the Río Tárcoles are preserved across the fan surface as inverted topographic ridges of welded tuff overlying river gravels ("snake flow" of Fisher et al., 1994; Marshall; 2000). Arc retreat and the resulting shift in the drainage divide may reflect the onset of flat subduction and the propagation of rough hotspot-thickened crust down the subduction zone (Marshall, 2000).

Fluvial terraces, coastal uplift, and fore arc segmentation

The correlation of fluvial and marine terraces (Fig. 14) across the Orotina coastal plain (Fig. 3, sites 3-5) provides a critical link for evaluating Quaternary uplift patterns across the subducting rough-smooth boundary (Marshall, 2000). These correlations (Fig. 14; Table 2) are constrained by spatial relationships between terrace flights, depostional characteristics, isotopic ages (^{14}C and $^{40}Ar/^{39}Ar$), and soil chronosequences based on B-horizon morphology and clast weathering rind thicknesses (Marshall, 2000). The overall uplift pattern along the Costa Rican coast (Fig. 15) strongly reflects the offshore bathymetry associated with the subducting Cocos Ridge and seamount domain (Gardner et al., 1992; Fisher et al., 1998).

The long-wavelength decrease in sea floor elevation northwest of the ridge axis (Fig. 15) is broadly consistent with the overall distribution of Quaternary uplift along the coast (Gardner et al., 1992). The highest measured uplift rates (6-7 m/ky) are from the Península de Osa, directly inboard

of the Cocos Ridge (Fig. 3, site 10). In contrast, the lowest uplift rates (~1 m/ky) are from the northernmost Península de Nicoya (Fig. 3, north of site 11). Shorter-wavelength roughness related to subducting seamounts superimposes local variability on the broad background uplift pattern, producing sharp elevation differences in Quaternary terraces between discrete coastal segments (Fisher et al., 1998; Marshall, 2000).

Along 150 km of coastline south of the rough-smooth boundary, major trunk rivers draining the volcanic arc flow along a system of regional-scale coast-orthogonal faults (Figs. 3). These steep faults segment the coastal fore arc into seven major blocks (Figs. 3 and 15) with sharply differing uplift rates (Fisher et al., 1994 and 1998). Mesoscale faults concentrated near block boundaries exhibit kinematics consistent with the observed vertical separation of Quaternary terraces across active block-bounding faults (Fisher et al., 1994 and 1998; Marshall et al., 2000).

North of the rough-smooth boundary, fluvial systems are symmetric with equal drainage areas on both sides of the trunk river (Figs. 3 and 15). However, all rivers to the south of the rough-smooth boundary show asymmetric drainage basins consistent with NW tilting about rotation axes parallel to the trunk streams (Fig. 15). This northwest-down tilting mirrors the long wavelength decrease in uplift rates along the coast northwest from the Cocos Ridge (Gardner et al., 1992).

The corrugated coastal uplift profile (Fig. 15), as expressed by sharp variations in terrace elevations, is similar to the short wavelength bathymetry of the seamount domain on the subducting plate (Fisher et al., 1998). For example, the Cabo Blanco, Herradura, and Quepos blocks (Fig. 3) show anomalously high uplift rates, and have a trench-parallel spacing and width comparable to incoming seamounts (Fig. 15). The similarity of the coastal uplift profile and the dimensions of offshore seamounts suggests that subducting plate roughness may directly impact deformation kinematics within the subaerial fore arc. Block uplift may result from the underplating of seamounts and net accumulation of mass beneath the coastal fore arc (Fisher et al., 1998).

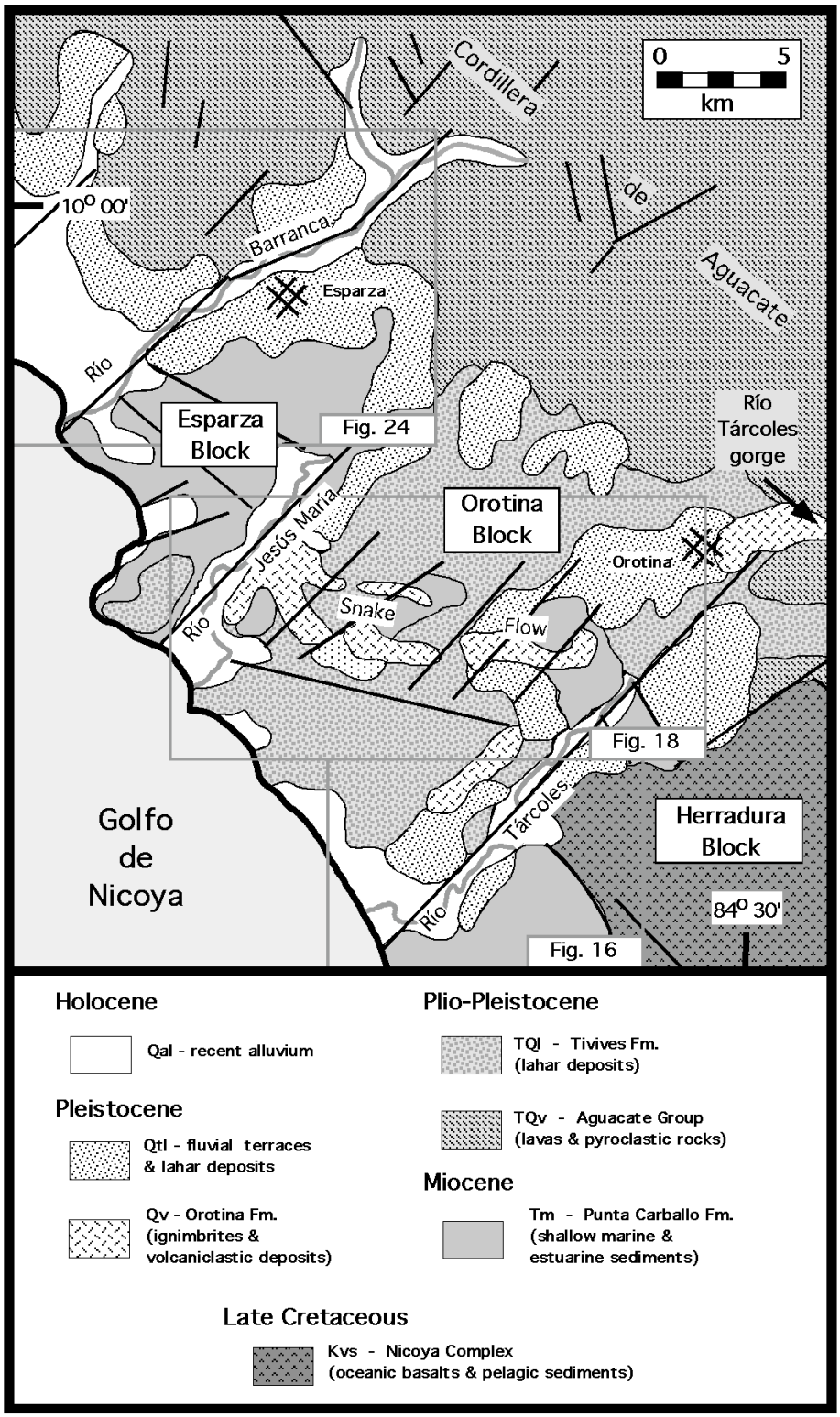

Figure 13. Geologic map of the Orotina debris fan along the central Pacific coast (from Marshall, 2000). Refer to Fig. 3 (sites 3-5) and Fig. 4 for location. Gray rectangles show detailed map areas of Figs. 16, 18, and 24. Straight solid lines indicate faults.

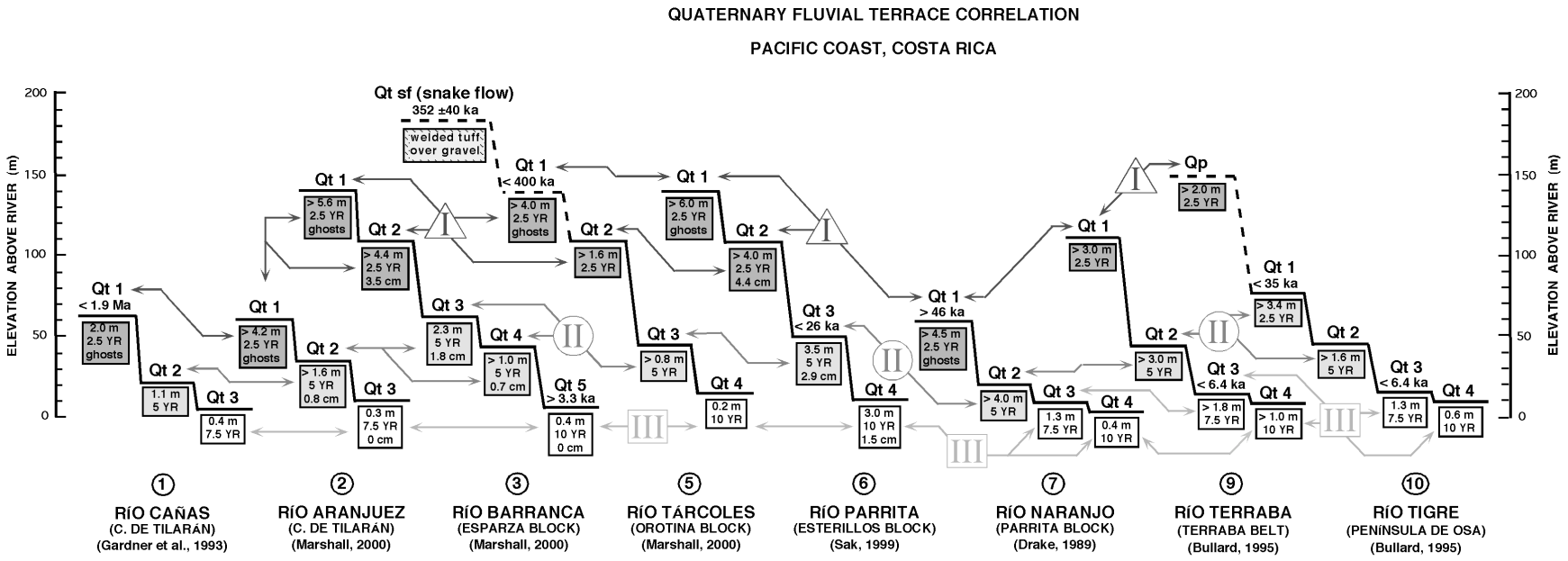

Figure 14. Summary of preliminary fluvial terrace correlations for selected Costa Rican Pacific coast rivers (from Marshall, 2000). Circled numbers above river names (bottom of figure) refer to locations shown on Fig. 3. Schematic terrace flight for each river shown by upward stepping black lines. Qt1-5 indicates local terrace designation for each river. Boxes display key soil morphologic data for each terrace: B horizon thickness, characteristic color, and average thickness of basalt clast weathering rinds. See Table 2 for complete data. Isotopic age constraints (e.g., ">46 ka") shown with respective terraces. Arrows indicate terrace correlations between rivers. Roman numerals, as well as gray shade of arrows and data boxes, indicate the three terrace correlation groups of Marshall (2000): Group I, dark gray; Group II, medium gray; Group III, light gray.

Table 2. Characteristic soil properties of fluvial and marine terraces, Pacific coast, Costa Rica & Nicaragua.
See Figure 3 for locations.

TERRACE			SOIL B HORIZON				WEATHERING RIND THICKNESS (cm)		TERRACE AGE	
no.	terrace group	surface name	thickness (cm)	color	ped structure	clay films	average	range	radiometric ages	inferred age range
				Cordillera de Tilarán						
1. Río Cañas*										
Qt1	I	El Diablo	200	2.5YR-10R	abk	4p	ghost	---	<1.9 Ma	80-240 ka
Qt2	II	Cañas	110	5-2.5YR	sbk	3p	---	---		25-60 ka
Qt3	III	San Pedro	35	10-7.5 YR	m	no	0	---		<7 ka
2. Río Aranjuez†										
Qt1	I	Bonilla (El Diablo)	420+	2.5YR-10R	3 abk	4p	ghost	---		80-240 ka
Qt2	II	Pipasa	160+	5 YR	2 abk	3-4p	0.8	0.3-1.5		25-60 ka
Qt3	III	Barbudal	30	7.5 YR	1 sbk	2f	0	---		<7 ka
				Orotina-Esparza coastal piedmont						
3a. Río Barranca (NW side)†										
Qt1	I	Esparza (El Diablo)	230+	2.5YR	3 abk	4p	ghost	---		100-240 ka
Qt2	I	Guatuso	260+	2.5YR	3 abk	3p	3.3	2.6-4.3		80-125 ka
Qt3	II	La Yunta	270	5-2.5YR	2-3 abk	3-4p	2.1	1.1-2.8		45-60 ka
Qt4	II	Hacienda Mango	90+	5YR	3 sbk	2d-3p	0.8	0.2-1.5		25-40 ka
3b. Río Barranca (SE side)†										
Qt1	I	Esparza (El Diablo)	560+	2.5YR-10R	3 abk	4p	ghost	---		100-240 ka
Qt2	I	Mojoncito	440+	2.5YR	3 abk	3-4p	3.5	2.7-4.6		80-125 ka
Qt3	II	Finca Machuca	230	5-2.5YR	2-3 abk	2d-4p	1.8	1.0-2.7		45-60 ka
Qt4	II	Pan de Azucar	100+	5YR	2-3 sbk	3-4p	0.7	0.1-1.4		25-40 ka
Qt5	III	El Peñon	35 (Bw)	10YR	1 sbk	no	0	---	3.3 ±0.2 ka	<7 ka
4. Río Machuca†										
Qt1	I	Orotina (El Diablo)	350	2.5YR	3 abk	4d	---	---		80-240 ka
Qt2	II	San Mateo	180	5 YR	2 abk	3-4d	0.8	0.5-1.1		25-60 ka
Qt3	III	Palenque	45	7.5 YR	2 sbk	3p	---	---		<7 ka
5a. Río Tárcoles (NW side)†										
Qtsf	---	Snake Flow	---	---	---	---	---	---	352 ±40 ka	312-392 ka
Qt1	I	Pozón (El Diablo)	400+	2.5YR	2-3 sbk	4p	ghost	---		100-240 ka
Qt2	I	Capulín	160+	5-2.5YR	2-3 sbk	3p	---	---		80-125 ka
Qt3	II	Garabito	80+	5YR	2 sbk	2d	---	---		25-60 ka
Qt4	III	Los Cocodrilos	20	10YR	1 sbk	no	0	---		<7 ka
5b. Río Tárcoles (SE side)†										
Qt2	I	El Barro	140+	5-2.5YR	2-3 sbk	2d-3p	---	---		80-125 ka
				Quepos-Parrita coastal piedmont						
6. Río Parrita††										
Qt1	I	Guapinol (El Diablo)	600+	2.5 YR	sbk	3	ghost	---		100-240 ka
Qt2	I	Loma	400+	2.5 YR	sbk	3	4.4	---		80-125 ka
Qt3	II	Tajo Bejuco	350	5 YR	sbk	2	2.9	---	>46 ka	25-60 ka
Qt4	III	Chires	300	10 YR	abk	2	1.5	---		<7 ka
7. Río Naranjo §										
Qt1	I	Naranjito (E.D.)	450+	2.5 YR	3 sbk	4p	ghost	---	>46 ka	80-240 ka
Qt2	II	Londres	450+	5 YR	2 sbk	4d	---	---		25-60 ka
Qt3	III	Finca Llorona	130	7.5 YR	3 sbk	4p	---	---		<7 ka
Qt4	III	Finca Cerros	40	10 YR	2 sbk	3f	---	---		<7 ka
				Valle del General						
8. Río El General §§										
Qt1	I	San Isidro	230	2.5YR-10R	2 sbk	---	---	---		100-240 ka
Qt2	I	Sta. Margarita	150+	2.5YR	2 sbk	---	---	---		80-125 ka
Qt3	II-III	Ceibo	210	5YR	2 sbk	4d	---	---	<17 ka	<17 ka
Qt4	III	Palmares	125	7.5-2.5YR	2 sbk	1f	---	---		<7 ka
Qt5	III	Hermosa	40	10 YR	m-1 sbk	---	---	---		<7 ka
				Terraba belt (Fila Costeña)						
9. Río Terraba #										
Qt1	I	Finca Marin	300+	2.5 YR	3 sbk	4p	---	---		80-240 ka
Qt2	II	Palmar Norte	300+	5 YR	3 sbk	3d	---	---		25-60 ka
Qt3	III	Palmar Sur	180+	7.5 YR	2-3 sbk	2f-3d	---	---		<7 ka
Qt4	III	Cajón	100+	10 YR	m-1 sbk	no	---	---		<7 ka
				Península de Osa						
10. Río Tigre #										
Qp	I		200+	2.5 YR	---	---	---	---		80-240 ka
Qt1	II		340+	2.5 YR	3 sbk	3-4p	---	---	<35 ka	25-60 ka
Qt2	II		160+	5 YR	3 sbk	4p	---	---		25-60 ka
Qt3	III		120+	7.5 YR	3 sbk	3-4p	---	---	6.4 ka	<7 ka
Qt4	III		60	10 YR	3 sbk	no	---	---		<7 ka
				Península de Nicoya						
11. Cabo Blanco†										
Qm1	I	Cobano	150+	2.5 YR	3 abk	4p	---	---		80-125 ka
				Nicaragua						
12. Huehuete†										
Qm1	I	La Boquita	110+	2.5 YR	3 sbk	4p	---	---		80-125 ka

* Gardner et al. (1993)
† Marshall (2000)
†† Sak (1999)
§ Drake (1989)
§§ Vaz Cabeda (1970); Kesel and Spicer (1985)
# Bullard (1995)

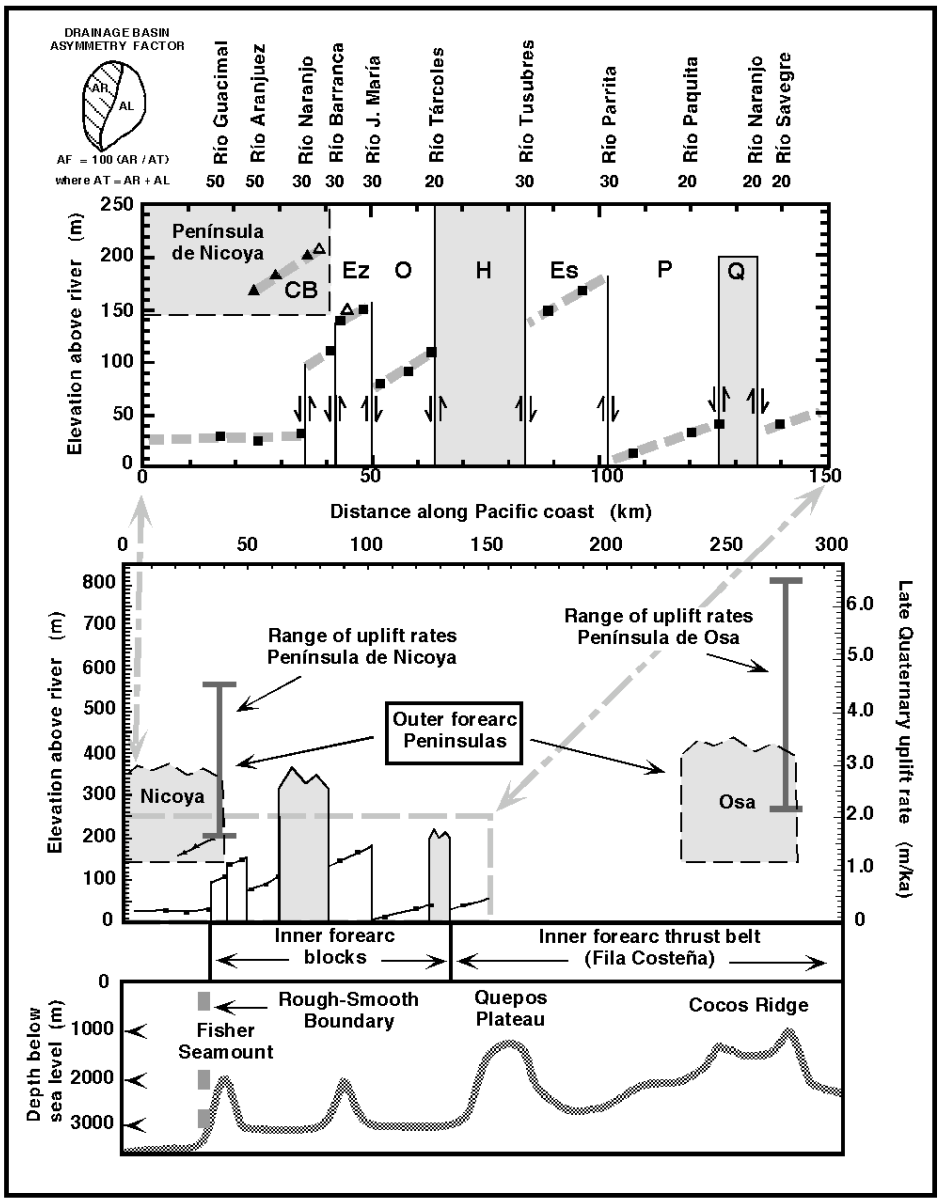

Figure 15. Central to southern Costa Rica, margin-parallel, Pacific coast schematic cross sections showing: inner fore-arc fault blocks and thrust belt, outer fore-arc peninsulas, coastal rivers with basin asymmetry factors, El Diablo fluvial terrace, Cóbano marine terrace, late Quaternary marine-terrace uplift rates, and offshore bathymetry (from Fisher et al., 1998 and Marshall, 2000). Upper plot: Close-up of fault blocks within inner fore arc and on southern edge of Península de Nicoya within outer fore arc. Inner fore-arc blocks: Ez-Esparza, O-Orotina, H-Herradura, Es-Esterillos, P-Parrita, Q-Quepos. Outer fore-arc block: CB-Cóbano. See Fig. 3 for locations. Solid squares-El Diablo terrace outcrops (6 km inland); dashed gray lines-projected El Diablo terrace surface; solid triangles-Cóbano marine terrace; open triangles-Holocene marine-platform uplift rates projected to expected elevation for a 125 ka terrace (oxygen isotope stage 5e sea-level highstand). Arrows indicate sense of vertical separation on block-bounding faults. Shaded blocks expose Cretaceous oceanic basement rocks (Nicoya Complex). Major coastal rivers shown above plot (AF-drainage basin asymmetry factor: AF = 50 indicates symmetric basin; AF < 50 indicates northwest-tilted block with larger basin area southeast of trunk river). Middle plot: Inner fore-arc fault blocks, Fila Costeña thrust belt, and outer fore-arc peninsulas (Nicoya and Osa). El Diablo terrace elevations (from detailed plot above) shown with range of late Quaternary coastal uplift rates for southern tips of Nicoya and Osa peninsulas (Marshall and Anderson, 1995; Gardner et al., 1992). Uplift rate scale (right side) corresponds with elevation scale (left side) for a 125 ka surface. Lower plot: Margin-parallel bathymetric profile across seamount domain and Cocos Ridge showing position of roughness elements with respect to fore arc.

Day 3 Field Trip Stops:

Stop 1. Río Tarcoles bridge - Fluvial terraces & Tárcoles fault

The Río Tárcoles (Fig. 3, site 5) represents the primary drainage for the Pacific slope of the active Cordillera Central volcanic range and the Valle Central basin of central Costa Rica. This river originates at the junction of the ríos Grande and Virilla in the western Valle Central and flows toward the Pacific coast along a deeply incised gorge through the extinct Miocene-Pleistocene Aguacate volcanic cordillera. The river exits the gorge onto the coastal piedmont (Fig. 13) and flows SW toward the ocean along a fault-controlled valley cut into the Orotina debris fan (Fig. 16).

Fluvial terrace development along the Río Tárcoles (Fig. 17) has been complicated by an apparent change in the river's course during the late Quaternary. Older river deposits extend westward across the upland surface of the Orotina debris fan outlining several paleo-river channels (Fig. 18). Subsequent terrace deposits occur along the incised SW-trending lower reach of the modern Río Tárcoles (Figs. 16 and 17). The youngest of these terraces are limited to the NW side of the river where it exits the canyon near the coast.

The NE striking Tárcoles fault (Figs. 13 and 16) accommodates vertical motion between the low-lying Orotina block and the uplifted Herradura block to the SE. The Herradura block, which contains the highest topography in the fore arc, exposes Cretaceous Nicoya Complex seafloor basalts which have been stripped of their sedimentary cover. While the Tárcoles fault forms the principal boundary between the Orotina and Herradura blocks (Fig. 13), several subsidiary faults (e.g., Carara and Turrubares) outline minor fault blocks along this trend. Vertical separation of up to 20 m for the Qt_2 fluvial terrace (minimum inferred age ~80 ka, oxygen isotope stage 5) implies active dip slip across this fault system at a maximum rate of 0.2 m/k.y. (Marshall, 2000).

Stop 2. Playa Bajamar seacliffs - framework of the Orotina debris fan

The Orotina debris fan originated with the deposition of multiple volcanic debris flows (Tivives Fm.; Madrigal, 1970) across the 25-km-wide coastal plain between Tárcoles and Barranca (Fig. 13). Individual lahar units may cover up to 200 km^2 and reach thicknesses in excess of 30 m. These large volume debris-flow deposits bury preexisting topographic relief on underlying Neogene deltaic sediments and volcanic rocks (Punta Carballo Fm. and Aguacate Group; Madrigal, 1970). The lahar deposits consist of a clay- and crystal-rich matrix that supports abundant clasts of diverse lithology, although dominated by basaltic andesites of the Aguacate Group. Clast sizes range from pebbles of several centimeters up to blocks reaching diameters >20 m.

Recent $^{40}Ar/^{39}Ar$ ages (Marshall and Idleman, 1999; Marshall, 2000) establish that the Tivives Fm. lahar deposits are predominantly early Pleistocene in age (1.7 - 0.9 Ma), and not Mio-Pliocene as previously mapped (Madrigal, 1970). Interbedded paleosols and fluvial sediments, abrupt changes in clast texture, and variations in matrix composition reflect the emplacement of separate flow units at 1.7 Ma, 1.4 Ma, and 1.1 Ma (Marshall, 2000).

The Tivives Fm. deposits are interpreted as eruption-generated volcanic debris flows (Marshall, 2000). Extensive lahar deposits are unique to the Orotina debris fan and do not occur elsewhere along the Costa Rican Pacific coast. These units, therefore, are not the product of regional denudation of the extinct volcanic cordillera, but instead represent localized events, such as explosive pyroclastic eruptions, centered in the Aguacate range above the Orotina debris fan.

The high clay content of these deposits suggests mobilization of hydrothermally-altered or weathered slope debris. However, the presence of abundant euhedral phenocrysts and intact juvenile pumice fragments within an ash-rich matrix also suggests a pyroclastic origin for these debris flows. Large blocks within the deposits are matrix supported and tend to be relatively intact, showing little evidence of shattering or brecciation typical of a cold, gravity-driven avalanche (e.g., Smith and Lowe, 1991). In addition, the presence of an inset welded tuff (Table 1; #17) with a nearly identical $^{40}Ar/^{39}Ar$ age to two of the lahar samples implies emplacement during explosive eruptions. These flows may be the products of sector collapse and surface water entrainment within major pyroclastic flows (e.g., Smith and Lowe, 1991). Field relationships suggest an origin within the Río Turrubares valley and westward flow onto the coastal lowland (Marshall, 2000).

Stop 3. Río Jesús María quarry - Quaternary volcanics & the snake flow tuff

Overlying the lahar fan (Fig. 18) is a sequence of ash flow tuffs, volcaniclastic sands, and fluvial gravels grouped together as the Orotina Fm. (Fig. 19; Madrigal, 1970). These materials occur as a thin veneer distributed across the underlying lahar deposits, as well as in moderately thick concentrations localized in topographic lows. A ryhodacitc welded tuff near the top of this sequence ("snake flow" of Fisher et al., 1994; Marshall, 2000) forms a set of sinuous ridges that trace meandering paleo-channels of the Río Tárcoles across the Orotina debris fan surface (Figs. 18, 20, 21, and 22). Due to the resistance of this unit relative to underlying lahar deposits, the snake flow has survived the erosional lowering of the surrounding landscape surface. An underlying horizon of river gravels defines the paleo-channel bottom, and hence preserves the longitudinal profile of the river (Fig. 22). Isotopic dating ($^{40}Ar/^{39}Ar$) of this deposit makes it a valuable tectonic timeline within the landscape. Measured offsets allow for the calculation of slip rates for steep forearc faults cutting the Orotina debris fan (Marshall, 2000).

Previous authors have proposed a link between the ignimbrites of the Valle Central and the ash flows of the Orotina debris fan (Dengo, 1960; Madrigal, 1970; Denyer and Arias, 1991). Recent field correlation supported by $^{40}Ar/^{39}Ar$ dating (Figs. 20 and 21; Table 1) confirmed this link (Marshall, 2000). The "snake flow" welded tuff on the Orotina debris fan (Fig. 18) can be traced from the coastal plain up the Tárcoles gorge into the Valle Central (Figs. 20 and 21) where it clearly merges with the Electriona member ignimbrites of the Avalancha Fm (Marshall, 2000).. The $^{40}Ar/^{39}Ar$ ages obtained for this unit from both the Valle Central (320, 331, 390 ka) and the Orotina debris fan (326, 352, and 373 ka) are statistically indistinguishable at the 2 sigma level (Table 1; Marshall, 2000).

Stop 4. Río Jesús Mária roadcut - Fault kinematics in the fore arc

The NE-striking Jesús María fault (Figs. 13 and 18) separates the uplifted Esparza block from the low-lying Orotina block to the SE. This fault forms a prominent SE-facing scarp along the NW bank of the Río Jesús María (Fig. 22). Pleistocene lahar deposits (Tivives Fm: age 1.42 ±0.13 Ma, $^{40}Ar/^{39}Ar$; Marshall 2000) and Miocene shallow marine volcaniclastic sediments (Punta Carballo Fm; Madrigal, 1970) are offset across the Jesús María fault with a NW-side-up separation of ~120 m (Fig. 22). This corresponds to a minimum dip separation rate of 0.08 m/k.y. for this block-bounding fault (Marshall 2000). However, if faulting began more recently than 1.4 Ma, as inferred for other block bounding faults, this rate may be higher.

In the roadcut just northwest of the Jesús María fault scarp, minor faults show dip-slip offset of Miocene volcaniclastic beds (Punta Carballo Fm.). Within the Costa Rican fore arc region, mesoscale faults display considerable variability in orientation and slip direction (Figs. 22 and 23; Marshall et al., 2000). Normal and strike-slip faults, however, significantly outweigh thrust faults in number and in magnitude of slip. Shallow *T* axes, combined with steep *P* axes, suggest a component of extension for most fault populations. This is consistent with offsets of Neogene-Quaternary units observed along steep, regional-scale, block-bounding faults (Figs. 22 and 23). Where mesoscale *P* and *T* axes are both shallow, the data show predominantly left-lateral motion on NE striking faults. This is consistent with sinistral transtension across the fore arc fault blocks.

Stop 5. Alto de las Mesas - Overview of fore arc fault blocks

Alto de las Mesas provides an outstanding view across the Orotina debris fan and fault blocks of the coastal fore arc region (Fig. 18). From the top of the Jesús María fault escarpment, the view extends to the SE from the edge of the Esparza block, across the coastal lowland of the Orotina block, to the towering peak of Cerro Turrubares on the Herradura block. The Esparza, Orotina, and Herradura blocks are prime examples of fault bounded segments of coastline experiencing moderate, low, and high rates of uplift respectively (Marshall, 2000).

Differing rates of block uplift - The relative magnitude of uplift within each segment of the coastal forearc can be evaluated based on several qualitative observations (Fisher et al., 1998; Marshall, 2000): 1) the topographic relief near the coastline, 2) the age of bedrock exposures (i.e., depth of unroofing), and 3) the elevation of the regionally extensive late Quaternary El Diablo fluvial terrace above modern river level. Where uplift rates are lowest (e.g., Orotina block), low relief (≤ 80 m) coastal plains expose primarily Quaternary sediments with minor exposures of older rocks, and the El Diablo terrace occurs at ≤80 m above river level . Along coastal segments experiencing moderate uplift (e.g., Esparza block), topographic relief within 5 km of the coast ranges from 80-180 m, bedrock exposures consist primarily of Tertiary sedimentary rocks, and the El Diablo surface occurs at ≥80 m above river level. Where uplift rates are highest, topographic relief within 5 km of the coast exceeds 180 m, oceanic basement rocks (i.e., Cretaceous Nicoya complex) are exposed, and the El Diablo terrace is absent.

Paleo-Río Tárcoles: Spillway for Valle Central ash flows - Also visible from Alto de las Mesas, is the source area of the Tivives lahars in the Turrubares Valley and the deeply incised Río Tárcoles gorge linking the Valle Central to the Orotina debris fan (Figs. 13 and 18). The Tárcoles gorge served as a spillway for pyroclastic flows descending from the Valle Central onto the coastal plain. The meandering ridges of the resistant "snake flow" tuff (Marshall, 2000) outline paleo-river channels that extend from the mouth of the Tárcoles gorge to the Jesús María fault scarp and Tivives estuary visible just below you (Fig. 18). Vertical offset along the Jesús María fault (prior to the snake flow) may have blocked the ancient river channel which previously reached the ocean through the modern underfit valley and estuary at Mata de Limón on the NW side of Alto de las Mesas (Marshall, 2000). After blockage, the river channel was deflected to the SW along the Jesús María fault, entering the ocean through the modern Tivives estuary. The resistant ridges of the snake flow welded tuff outline this later pathway (Fig. 18).

Faults of the Orotina block & the 1924 Orotina earthquake - The interior of the Orotina block (Figs. 18 and 22) is cut by a sequence of minor (<5 km length) NE-striking faults (Tivives, Trinidad, Diablo, Pozón and Coyote). These faults exhibit dip-slip offset of late Quaternary ash flows, volcaniclastic sediments, and fluvial terrace gravels of the Orotina Fm. (Fig. 18 and 20). This deformation has generated a system of horsts and grabens that expose Miocene sediments and Plio-Pleistocene lahar deposits within isolated topographic highs (Fig. 22). These faults have produced up to 50 meters of vertical displacement along the longitudinal profile of the snake flow welded tuff (~350 ka, $^{40}Ar/^{39}Ar$). Rates of dip separation range from 0.03 m/k.y. to 0.14 m/k.y. across these faults (Marshall, 2000). Minor lateral displacements are more difficult to constrain due to the discontinuous nature of remaining snake flow deposits.

Historically, shallow upper plate earthquakes within the fore arc have been relatively rare in comparison to the volcanic arc and back arc. A seismic sequence in 1989 centered on the coastal piedmont of the Orotina block (Fig. 22) showed oblique-normal slip along a linear NE trend (Güendel et al., 1989). This swarm occurred in the same location as the *M*=7.0 Orotina earthquake of 1924, which caused extensive damage in central Costa Rica. According to eyewitness interviews, the 1924 event produced a 4-km-long NE trending ground rupture west of the town of Orotina (Güendel et al., 1989). Additional interviews with local residents (Marshall, 2000) confirmed this observation and suggested a location for this rupture along Quebrada Pozón (Fig. 18, ~4 km west of Orotina). The location and trend of both the 1924 ground rupture and the 1989 seismic swarm correspond with those of the Diablo and Pozón faults (Figs. 18 and 22; Marshall, 2000). The 1989 composite focal mechanism, the 1924 ground rupture, mapped Quaternary offsets, and mesoscale fault data (Fig. 22) are all consistent with transtension accommodated by oblique slip mostly along NE striking margin-perpendicular faults within the inner fore arc (Marshall et al., 2000).

Stop 6. Mata de Limón estuary - Ancient river mouth of the Río Tárcoles?

In the early Pleistocene, aggressive stream piracy across the crest of the Aguacate range led to the progressive capture of watersheds within the newly formed Valle Central basin. The rapid elaboration of an extensive river network feeding toward the Tárcoles gorge redirected Valle Central drainage to the Pacific coastal plain (Fig. 3). The lower trunk segment of the Río Tárcoles had incised a channel into the Orotina debris fan (Fig. 13 and 18) flowing westward along the ancestral path of the Río Turrubares to a river mouth near the modern estuary of Mata de Limón (Puerto Caldera). While fluvial terrace deposits are not apparent in the wind gap between the Río Jesús María and Mata de Limón (Fig. 18), the headless coastal embayment and underfit stream valley at Mata de Limón strongly suggest association with a major river channel (Marshall, 2000). By 400 ka, vertical displacement along the Jesús Mária fault (NW side up) formed an obstruction for the Río Tárcoles, redirecting its lowest reach into the area of the modern Tivives estuary.

Stop 7. Río Barranca overlook - The Barranca fault & the El Diablo terrace

A well-developed flight of five fluvial terraces (Figs. 23, 24, and 25) occur along the lower reaches of the fault-controlled Río Barranca (Fig. 3, site 3). Vertical offsets of up to 30 m across the Río Barranca (Fig. 23) and up to 4 m for Holocene marine benches near the river mouth demonstrate active slip along the Barranca fault (Fisher et al., 1994 and 1998; Marshall, 2000). A radiocarbon date of 3.3 ± 0.2 ka for wood beneath a colluvial wedge on the uplifted Holocene platform indicates a maximum late Holocene uplift rate of 1.3 m/k.y. for the Esparza block near the Barranca fault (Marshall, 2000). This rate is consistent with longer-term average uplift of the Barranca fluvial terraces at rates of 0.7-1.7 m/ky Remnants of the upper three terraces (Qt_{1-3}) on opposite sides of the Barranca fault (Figs. 23, 24, and 25) show the same magnitude of vertical offset (~30 m). This observation suggests that slip along the fault is relatively recent, having begun after formation of Qt3. Based on an inferred age range of 45-60 ka (oxygen isotope stage 3) for Qt3, we estimate a vertical separation rate of 0.5-0.7 m/ky for the Barranca fault (Marshall, 2000).

The El Diablo surface - The upper terrace at Barranca, referred to as the "El Diablo surface" (Fisher et al., 1994 and 1998; Marshall, 2000), forms an extensive upland mesa on both sides of the Río Barranca covering a total area of nearly 20 km^2 (Fig. 24). This large aggradational deposit has been referred to by previous authors as the "Red boulder-clay" (Hill, 1898), the "Terraza de Esparta" (Dondoli, 1958), the "Formación Esparza" (Madrigal, 1970), and the "Meseta de Esparza" (Kruckow, 1974). The El Diablo terrace deposit consists of a highly weathered, massive river gravel of up to 50 m in thickness. Gravel clasts typically range in size from 5-20 cm, with rare boulders > 1m. Except for the largest boulders, all gravel clasts are weathered entirely to clay ghosts. The soil formed on this deposit exhibits a highly distinctive, bright red (2.5 YR-10R) Bt horizon that exceeds 5 m in thickness with prominent clay films (Table 2; Marshall, 2000).

Based on its distinctive characteristics, the El Diablo surface can be correlated with other extensive, deeply-weathered terraces recognized along most Pacific slope drainages in Costa Rica

(Fig. 14; Table 2; Gardner et al., 1993; Fisher et al., 1994 and 1998; Marshall, 2000). This pervasive, regionally-extensive terrace provides an important geomorphic surface for evaluating coastal uplift patterns along the Costa Rican margin (Fig. 15).

Valley aggradation during sea level rise toward eustatic highstands commonly builds an alluvial prism within the lower reaches of coastal rivers (e.g., Merritts et al., 1994; Talling, 1998; Blum and Törnqvist, 2000). Along active tectonic margins, progressive uplift will result in the emergence and abandonment of aggradational surfaces formed during past highstands. The pervasive deeply weathered El Diablo fill terrace, found along all major river systems of Costa Rica's central and northern Pacific coast, is interpreted as an abandoned composite alluvial prism formed during sea level rise toward eustatic highstands of the late Quaternary (Fig. 26; Marshall, 2000). Lower terraces, inset below the El Diablo surface (e.g., Figs. 24 and 25) may also reflect valley aggradation during sea level rise. Isotopic age constraints (Table 2) and the correlation of terrace surfaces with sea level curves (Fig. 26) allows for the estimation of age ranges for fluvial terrace sequences (Fig. 14; Table 2; Marshall, 2000). These age ranges provide important constraints for evaluating relative uplift rates (Fig. 15) and rates of weathering rind growth on basalt gravel clasts (Fig. 27; Fisher et al., 1994 and 1998; Marshall, 2000; Sak et al., in review). The relative thickness of weathering rinds developed on basalt gravel clasts has been used as an effective parameter for correlating terrace deposits between drainages along the Pacific coast (Fisher et al., 1998; Marshall, 2000). Limited isotopic age constraints coupled with numerical models for weathering rind kinetics (Sak et al., in review), may provide an important future tool for evaluating terrace ages along the entire Costa Rican margin.

Regional terrace correlation - A preliminary framework for regional terrace correlation along the Costa Rican coast (Fig. 14; Marshall, 2000) assigns each surface to one of three terrace groups: Group I, Late Pleistocene (oxygen isotope stages 7-5, 240-80 ka); Group II, Late Pleistocene (stage 3, 60-25 ka); and Group III, Late Holocene (stage 1, <7 ka). While the three terrace groups (I-III) are a common feature of all Pacific slope rivers, the total number of terraces in each group varies between drainages with respect to the relative magnitude of block uplift (Figs. 14 and 15). This relationship suggests that terrace generation is strongly controlled by the interaction of rock uplift and eustatic sea level fluctuation (Pazzaglia et al., 1998; Marshall, 2000). Where uplift rates are low (e.g., northern Pacific slope), each of the three terrace groups is represented by a single surface. Along the central coast, fault blocks experiencing moderate uplift (e.g., Esparza, Orotina, Esterillos) preserve the highest number of terraces, with multiple surfaces in each terrace group corresponding with discrete sub-stage highstands (e.g., 5a and 5e) of each interglacial period. Moderate uplift rates along these coastal segments are high enough to produce vertical resolution of substage surfaces, but not high enough to cause the loss of the older surfaces to erosion. Where uplift rates are highest (e.g., Herradura block and Península de Osa), the older terraces (Group I) are absent, having been consumed by erosion at elevations above an optimum zone of terrace preservation (analogous to the "marine terrace fringe" of Anderson et al., 1999).

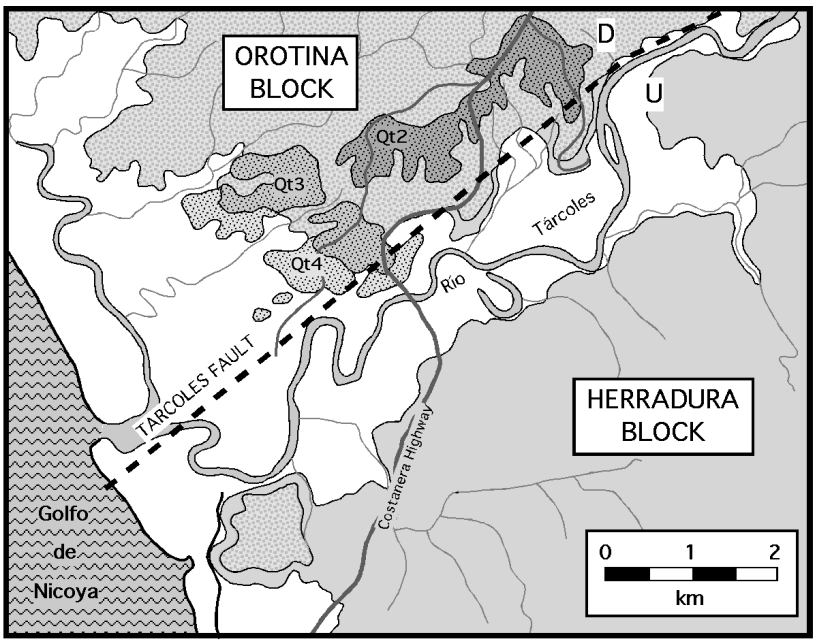

Figure 16. Geologic map (from Marshall, 2000) showing the distribution of fluvial terraces along the lower Río Tárcoles (Fig. 3, site 5). Map location shown on Fig. 13 by solid gray rectangle. Heavy black lines mark faults with relative vertical displacement indicated by U, up and D, down. Thin light gray lines outline rivers and medium dark gray lines indicate roads.

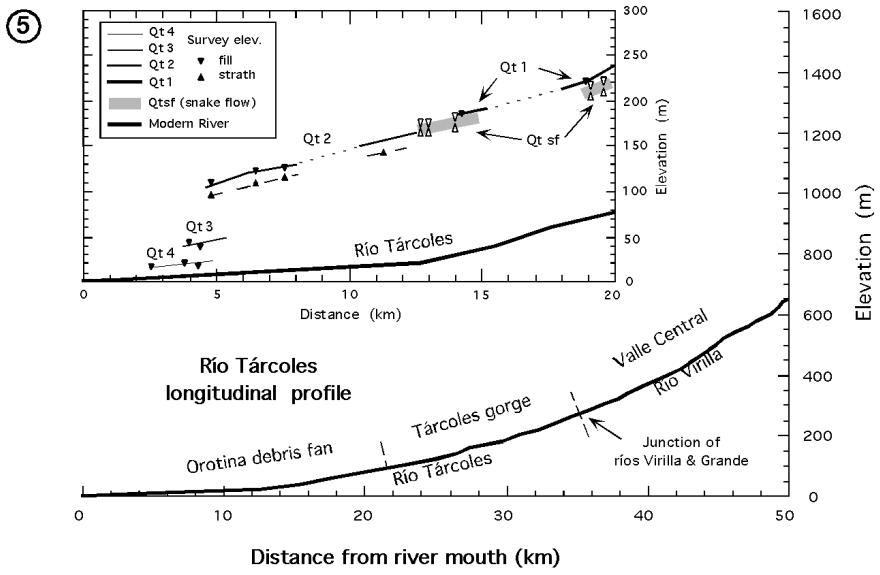

Figure 17. Fluvial terrace longitudinal profile reconstructions (from Marshall, 2000) for the Río Tárcoles (Fig. 3, site 5). Large outer plot shows extended modern river profile. Small inner plot shows terrace long profiles along detailed lower segment of the modern river. See Table 2 for terrace characteristics and age constraints. Longitudinal profile reconstructions based on techniques outlined by Merritts et al. (1994).

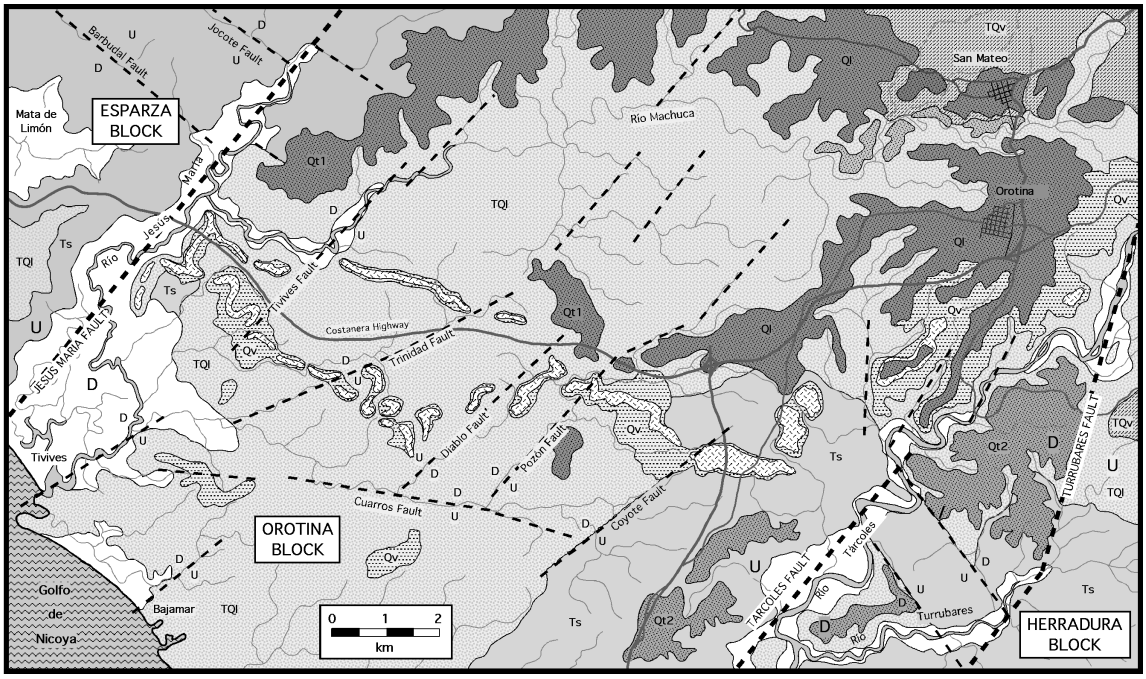

Figure 18. Geologic map of the Orotina block (from Marshall, 2000) showing the distribution of fluvial terrace deposits associated with the ríos Machuca and Tárcoles (Fig. 3, sites 4 and 5). Paleo-channels of the Río Tárcoles are outlined by the snake flow welded tuff (Qv). Map location shown on Fig. 13 by solid gray rectangle. Heavy black lines mark faults with relative vertical displacement indicated: U, up; D, down. Thin light gray lines outline rivers and medium dark gray lines indicate roads.

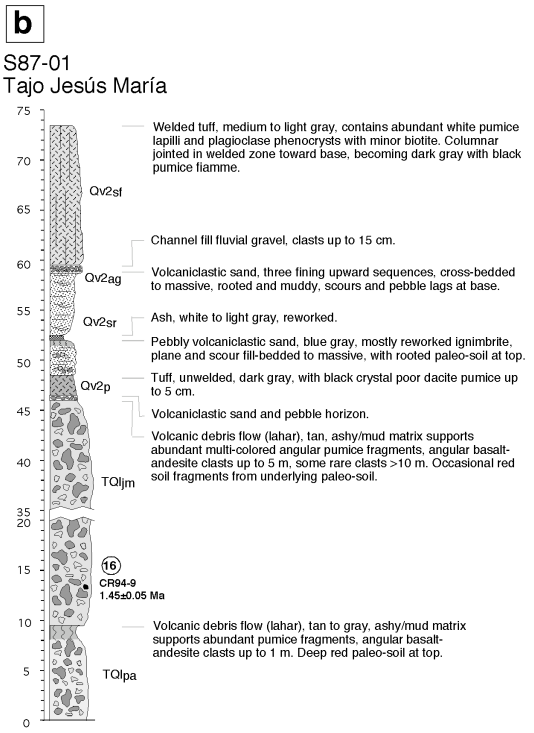

Figure 19. Stratigraphic column (from Marshall, 2000) for the Jesús María quarry showing local exposure of the Quaternary volcanic units of the Orotina debris fan (Orotina and Tivives Fms.; Madrigal, 1970) See Figs. 20 and 21 for location and stratigraphic correlation. Numbered circle indicates location of 40Ar/39Ar dated sample.

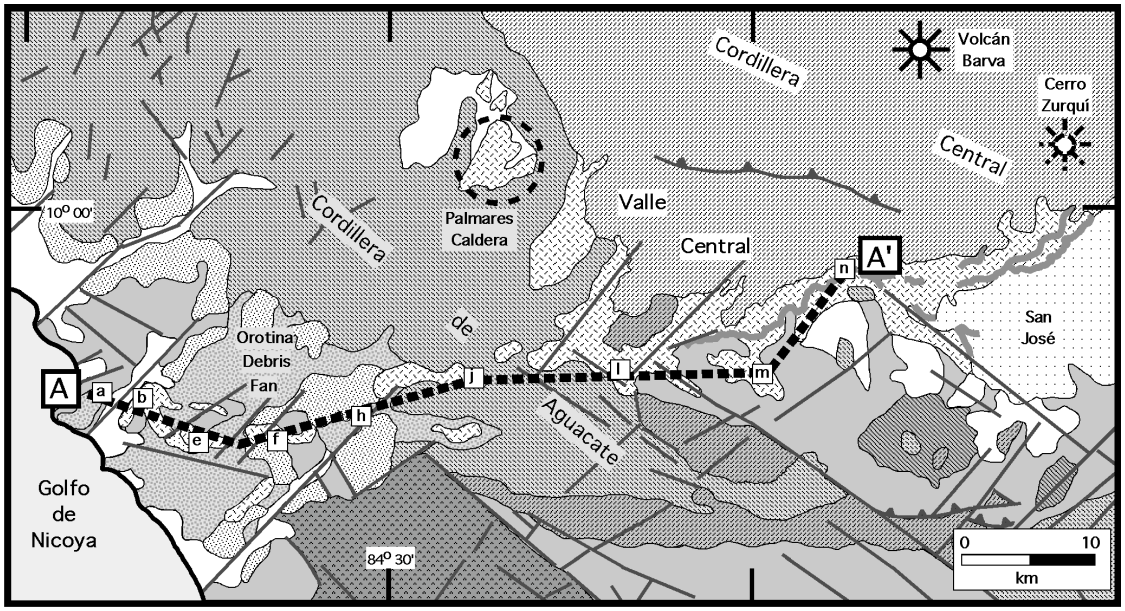

Figure 20. Geologic map (from Marshall, 2000) showing the locations of stratigraphic columns in Fig. 21 (small lettered squares) and correlation line (dashed) linking Quaternary volcanic units of the Orotina debris fan with those of the Valle Central. See Fig. 4 for geologic map explanation.

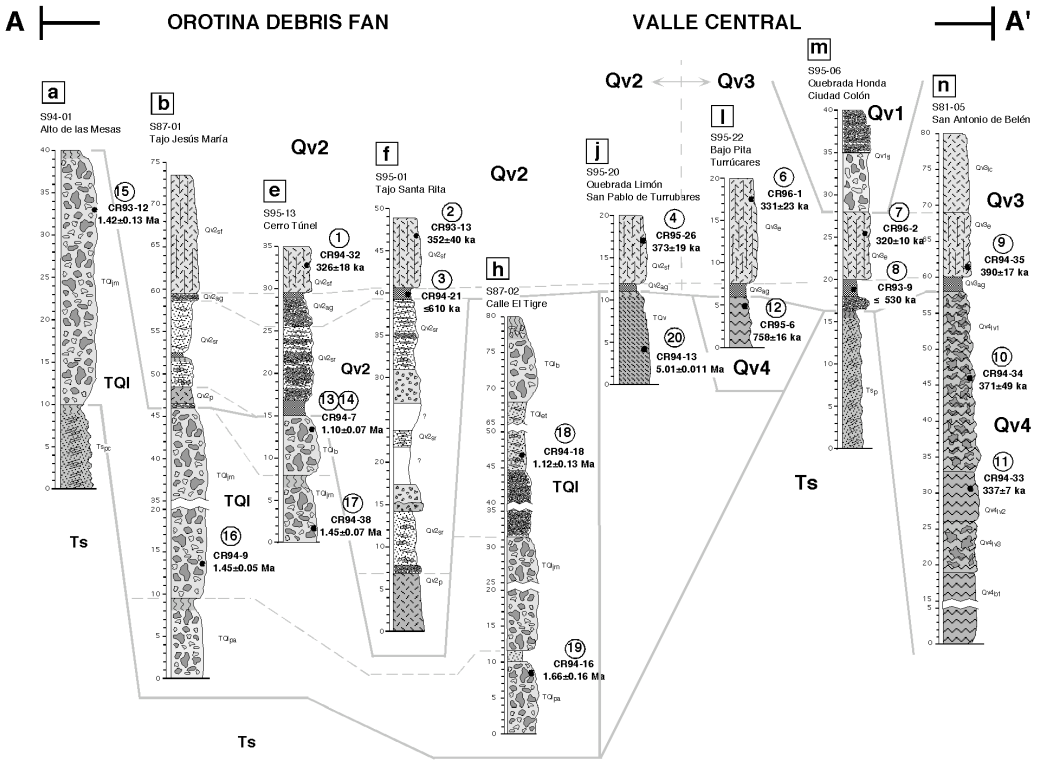

Figure 21. Stratigraphic columns (from Marshall, 2000) showing Quaternary volcanic units of the Orotina debris fan and Valle Central. Lettered squares correspond with locations shown on Fig. 20. Numbered circles adjacent to columns mark the locations of 40Ar/39Ar dated samples (See Fig. 5 and Table 1 for context and complete data). Solid gray lines: formation boundaries; dashed gray lines: member boundaries.

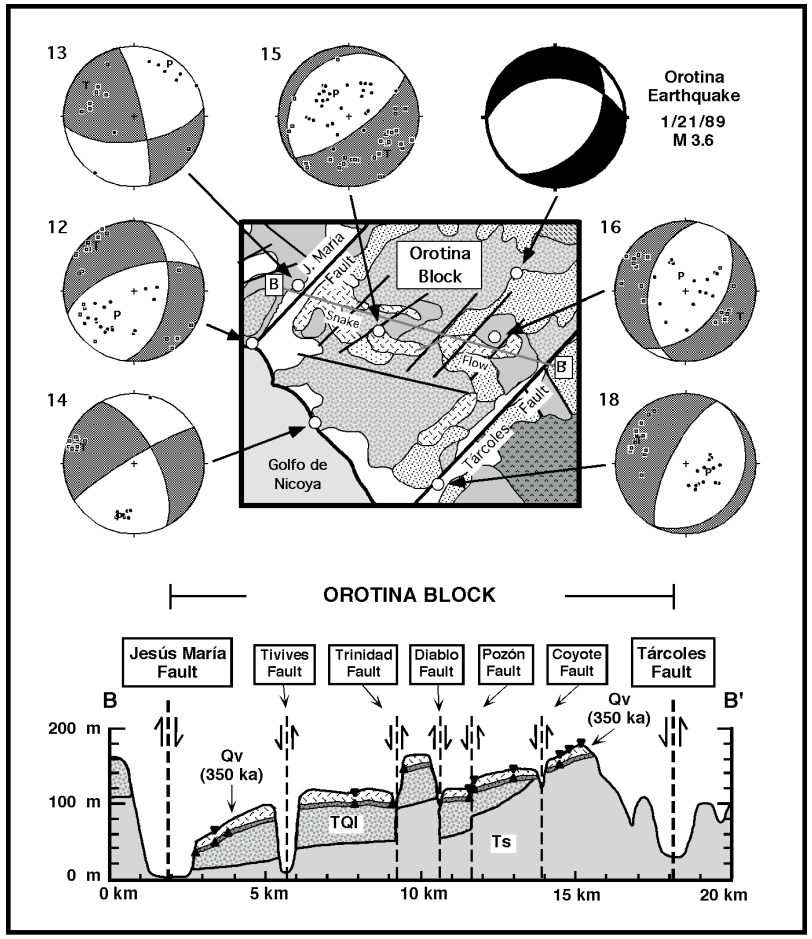

Figure 22. Geologic map and cross section for Orotina block (from Marshall, 2000) showing active faults, mesoscale fault data, and an earthquake focal mechanism (1989 M3.6). Straight solid lines indicate faults. Cross section location depicted on map by lettered gray lines. Mesoscale fault data from Marshall et al. (2000) and earthquake focal mechansim from Güendel et al. (1989). See Fig. 13 for location and explanation of geologic units. See Fig. 18 for detailed geology.

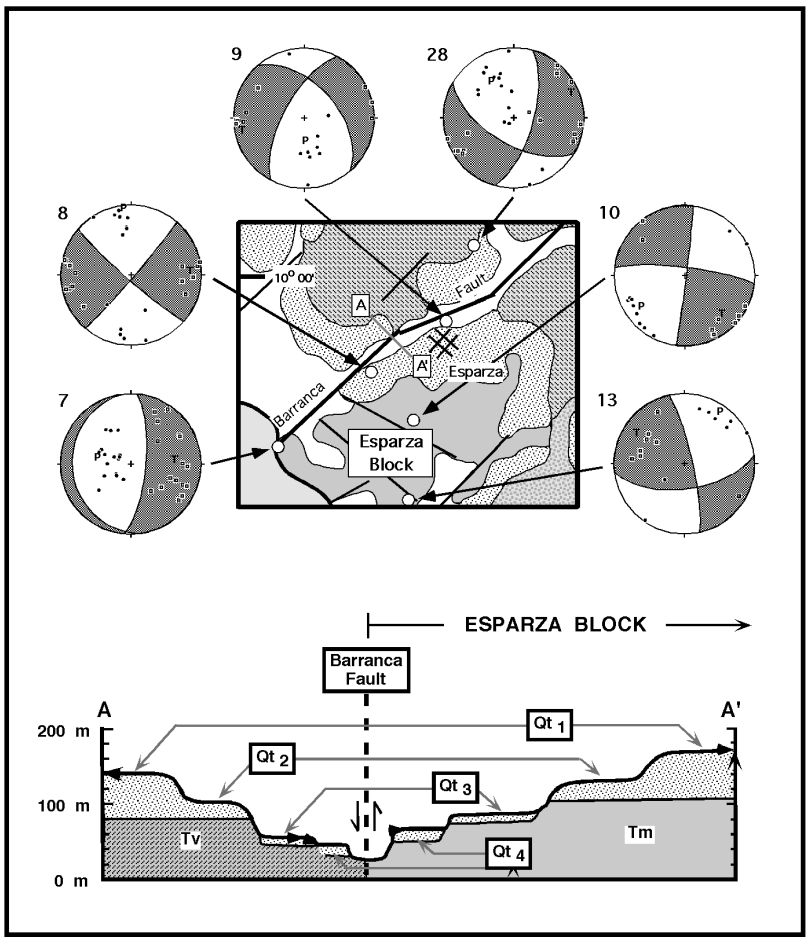

Figure 23. Geologic map and cross section for Esparza block showing active faults and mesoscale fault data. Straight solid lines indicate faults. Cross section location depicted on map by lettered gray line. Mesoscale fault data from Marshall et al. (2000). See Fig. 13 for location and explanation of geologic units. See Fig. 24 for detailed geology.

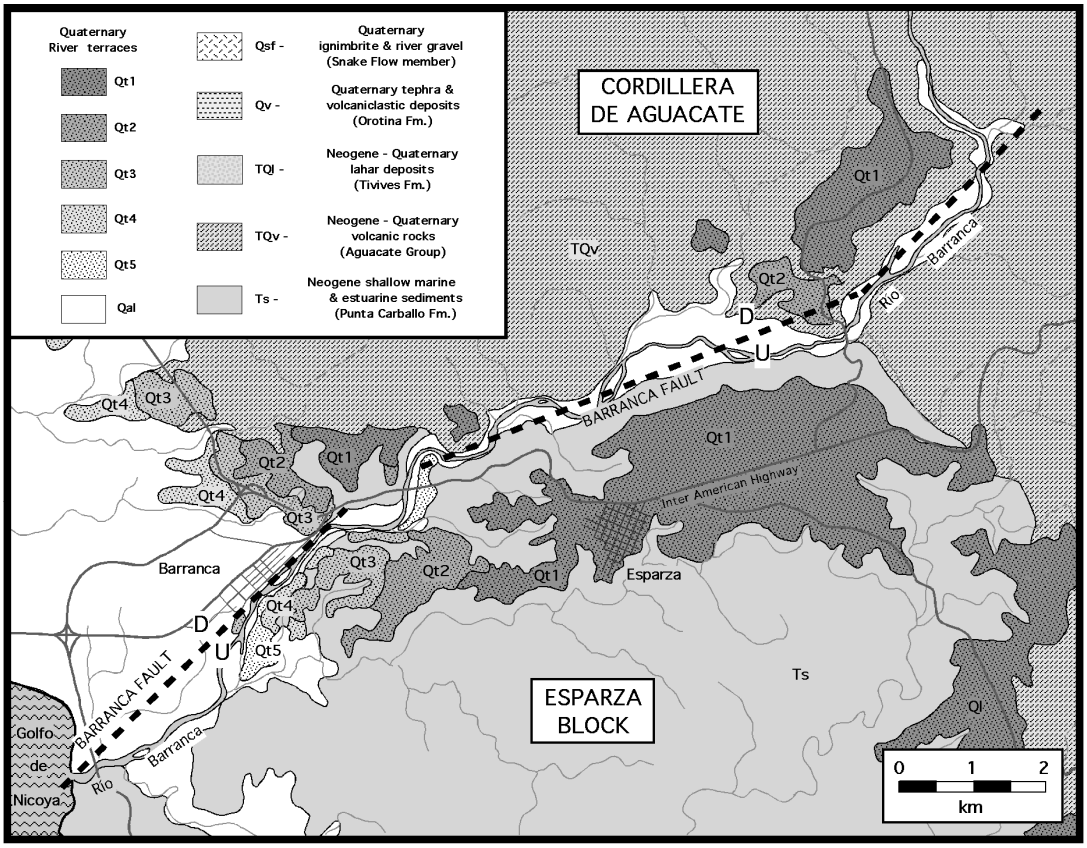

Figure 24. Geologic map of the northwestern Esparza block (from Marshall, 2000) showing distribution of fluvial terraces along the Río Barranca (Fig. 3, site 3). Map location shown on Fig. 13 by solid gray rectangle. Heavy black lines mark faults with relative vertical displacement indicated by U, up and D, down. Thin light gray lines outline rivers and medium dark gray lines indicate roads.

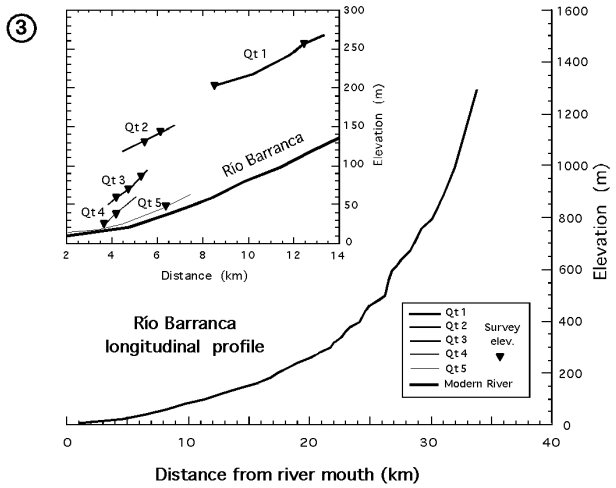

Figure 25. Fluvial terrace longitudinal profile reconstructions (from Marshall, 2000) for the Río Barranca (Fig. 3, site 3). Large outer plot shows extended modern river profile. Small inner plot shows terrace long profiles along detailed lower segment of the modern river. See Table 2 for terrace characteristics and age constraints. Longitudinal profile reconstructions based on techniques outlined by Merritts et al. (1994).

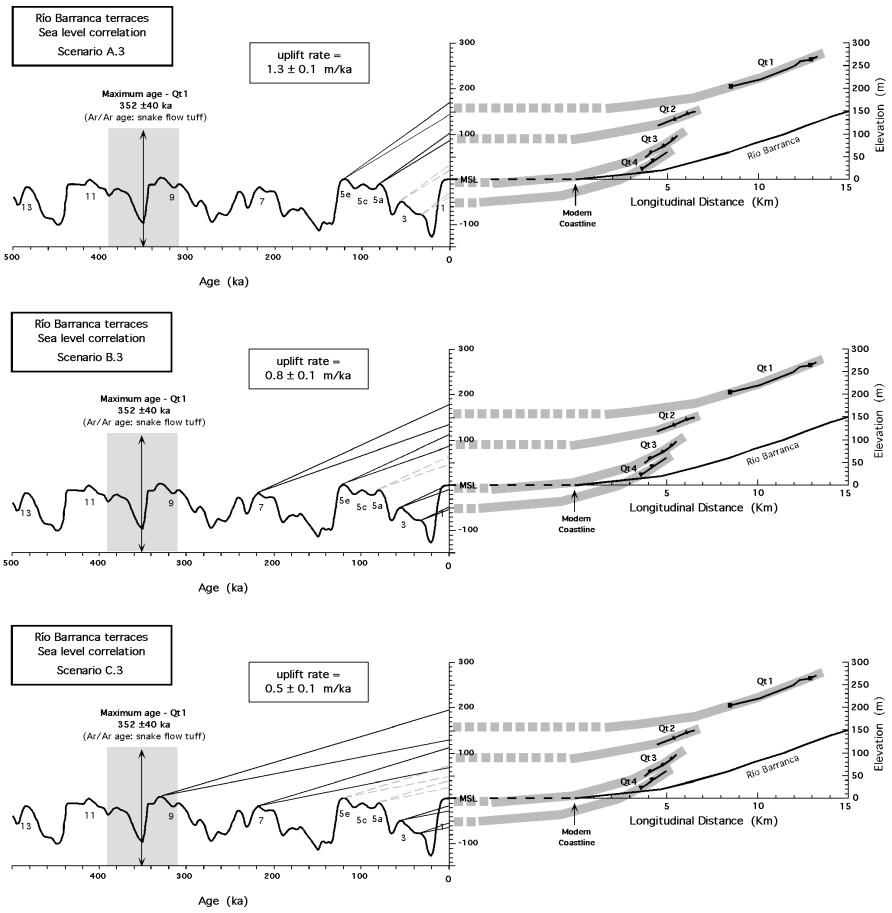

Figure 26. Sea level correlation diagrams for terrace longitudinal profiles of the Río Barranca (from Marshall, 2000). The right-hand plot of each diagram shows terrace profiles (solid black lines) from Fig. 24. The left-hand plot depicts late Quaternary eustatic sea level (modified after Shackleton and Opdyke, 1973; Imbrie et al., 1984; Anderson et al., 1999). Solid gray curves represent ideal projections of terrace long profiles, with dashed gray lines marking paleo-base levels. Three correlation scenarios (A-C) are based on matching the Qt1 terrace with each of the three major sea level high stands (stages 5e, 7, and 9) subsequent to 352 ka (Qt1 maximum age). Lines connecting sea level highstands with terrace base levels on the vertical axis represent uplift pathways, with the slope of the line equivalent to the uplift rate (e.g., Bull, 1985; Lajoie, 1986; Bloom and Yonekura, 1990; Gardner et al., 1992). Two lines projected from each highstand outline a ±1.0 m/ky envelope about the respective uplift rate. This model assumes a constant rate of rock uplift through time.

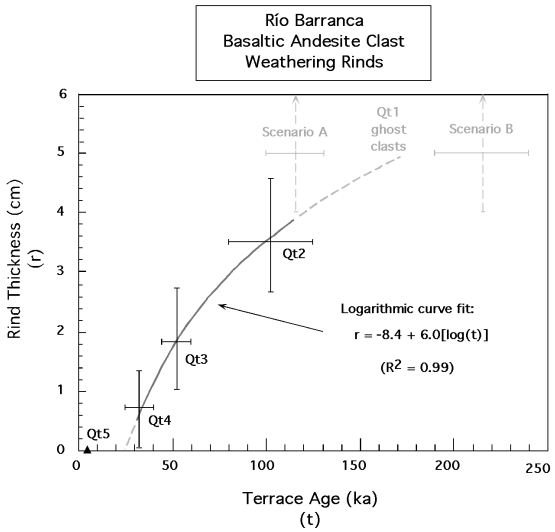

Figure 27. Plot of the thickness of basalt clast weathering rinds versus inferred terrace age for Río Barranca terraces (from Marshall, 2000). The range of rind thicknesses for each terrace is based on the range of measured clast samples (see Table 2). Data for Qt1 shown in grey to reflect uncertainty of rind thickness (ghost clasts). The terrace age ranges are derived from sea level curve correlations (Fig. 26). The two possibilities for the age of Qt1 (A and B) correspond with sea level correlation scenarios A and B. The best fit curve for the data describes a logarithmic time function for the rate of weathering rind growth.

DAY 4:

Sunday, 8 July 2001

Quaternary geology and tectonics of the Herradura, Esterillos, Parrita, and Quepos Blocks

Road Log (Day 4):

This morning we will drive south along the Costanera highway to explore the Quaternary geology and tectonics of a series of coastal fault blocks to the southeast of the rough-smooth boundary (Herradura, Esterillos, Parrita, and Quepos (Fig. 3). As we leave Villa Lapas and proceed toward the village of Tárcoles, the highway runs along the mountain front of the rapidly uplifting Herradura block (Fig. 28). Where the highway reaches the ocean, at the fishing hamlet of La Pita, we will have view to the southeast along a steep, fault-controlled segment of coastline running orthogonal to the margin. A series of similar coastal segments form the boundaries of rocky headlands and bays along the coast of the Herradura block (Fig. 28). Rocky intertidal platforms and cliffs along this coastline exhibit an abundance of mesoscale faults showing kinematics consistent with observed slip on steep, regional-scale block bounding faults (Fig. 28).

Continuing southeast from La Pita, we turn inland and climb a steep ridge (Cuesta Chiquero), gaining an excellent view to the northwest up the axis of the Golfo de Nicoya. As the road descends from the ridge top, we pass through roadcuts exposing Tertiary marine sediments draped along the seaward margin of the rapidly uplifting Herradura block. The rugged, mountainous interior of the Herradura block visible to the northeast, exposes primarily oceanic basalts of the Nicoya Complex, its Tertiary sedimentary cover having been eroded off of this topographic high.

The road continues along the inland edge of the bays and headlands of Herradura and Jacó, reaching the ocean again at Punta Guapinol, just southeast of Playa Jacó (Fig. 28). A stop here provides a look at roadcut exposure of the highly deformed pillow basalts of the Nicoya Complex. Rounding the point, we have a view to the southeast along the expanse of Playa Hermosa, one of Costa Rica's premiere surfing beaches (Fig. 28). This beach is formed across the extensive estuary of the Río Tusubres, a major trunk river flowing along the coast-orthogonal fault separating the Herradura and Esterillos blocks (Fig. 29). The road swings inland and crosses the river onto the Esterillos block, passing through subdued hills formed on Neogene shallow water sediments and capped by Pleistocene fluvial terrace gravels.

At the village of Esterillos Oeste, we will turn off the highway and walk out along the intertidal platform at Punta Judas (Fig. 30). This platform exposes faulted, fossiliferous beds of Neogene shallow marine to estuarine sediments, and is another excellent location to view the active process of marine terrace formation. Faults and joints on this surface reveal an evolving deformation history along the central Costa Rican margin.

After lunch at Punta Judas, we continue southward on the Costanera highway, skirting along the seaward edge of the Esterillos block (Fig. 31), past abundant exposures of Pleistocene terrace gravels (watch for the deep red soils). Near Bejuco, we will turn inland, passing through palm oil plantations, and climb into the interior of the Esterillos block past a sequence of fluvial terraces associted with the Río Parrita. This major river marks the fault boundary between the Esterillos and Parrita blocks. At Alto Guapinol, we will stop and enjoy an excellent view from the top of the El Diablo terrace, southeastward across the coastal lowlands of the Parrita block. The fluvial terraces at this site are offset across the Parrita fault and correlated with low-elevation flights of terraces formed on rivers draining the Parrita lowland. The Quepos block, a small, isolated coastal headland visible in the distance, marks a point of localized coastal uplift. The view also encompasses the northern Fila Costeña, a steep, linear coastal mountain range formed along the Terraba thrust belt, inboard of the subducting Cocos Ridge.

Retracing our route back to the Costanera highway, we return to the northeast, back toward the rugged coastal headland of the Herradura block. After passing Playa Herradura (Fig. 28), we will again climb the ridge of Cuesta Chiquero, turning off to visit the spectacular mountain top hotel of Villa Caletas. We will stop here and enjoy refreshments while taking in the tremendous view of Golfo de Nicoya and the rugged coastline onshore of the subducting rough-smooth boundary.

Geologic Overview (Day 4):

See second half of overview for Day 3.

Day 4 Field Trip Stops:

Stop 1. Punta Guapinol (Jaco) - Oceanic basement of the Herradura block

A steep, northeast-striking fault along the Río Tárcoles marks the primary boundary between the Orotina and Herradura blocks (Fig. 28). This margin-perpendicular fault juxtaposes Neogene shallow-marine sediments and Quaternary volcanic rocks of the Orotina block against Cretaceous oceanic basement rocks of the Nicoya Complex on the Herradura block (Fisher et al., 1998). The Herradura block coincides with the highest topography along the central Pacific coast. Rapid uplift and unroofing has exposed the basement rocks and stripped the Herradura block of most of its Tertiary and Quaternary cover (Fisher et al., 1998). The oceanic basalts and radiolarites exposed along the coastline of the Herradura block belong to an uplifted fragment of the Cretaceous Caribbean Oceanic Plateau (Donelly, 1994; Arias, 2000). Within the interior of the Herradura block, these basement rocks are overlain by Late Cretaceous-early Teritiary oceanic island basalts and epiclastic sediments of the Tulín Fm. (Arias, 2000).

Stop 2. Punta Judas - Changing stress orientations above subducting seamounts

A rocky intertidal platform at Punta Judas on the Esterillos block (Fig. 29) provides structural evidence of two discrete late Cenozoic deformation events along the central Costa Rican margin (Sak, 1999). This ~4 km long and ~1 km wide abrasion platform is cut into mid-Miocene estuarine sediments of the Punta Judas Fm. (Fig. 30; Haller and Protti, 1987; Seyfried et al., 1994). An early deformation, characterized by sub-vertical joints that strike at low angles to the MAT, might be indicative of gravity-driven layer-parallel extension within upper slope sediments (Fig. 30; Sak, 1999). Downslope extension is prevalent in seismic reflection profiles offshore of the Nicoya Peninsula that show numerous trenchward dipping normal faults that displace sediments of the upper slope, some of which displace the seafloor (McIntosh et al., 1993). This deformation is overprinted by a more recent deformation characterized by sub-vertical, northeast-southwest striking joints that evolve into mesoscale faults with strike-slip displacements (Fig. 30; Sak, 1999). This later deformation, characterized by trench-parallel extension, is common in the portions of the fore arc overriding the seamount domain on the Cocos plate (Fisher et al., 1998; Marshall et al., 2000). Evidence for both of these deformations has also been observed offshore through seismic imaging and drilling of the lower slope sediments.

The presence of the second joint set at Punta Judas suggests a stress reorientation from a subhorizontal s3 orientation perpendicular to the MAT to a subhorizontal s3 orientation parallel to the MAT (Sak, 1999). The northeast-southwest striking joints show a progressive evolution from isolated joints segments to en echelon arrays. All stages of this evolution can be observed. Fracture patterns record a progressive evolution from distributed jointing to concentrated jointing along conjugate zones to development of conjugate strike-slip faults that cut the entire platform and record meter-scale displacements (Fig. 30; Sak, 1999).

Stop 3. Alto Guapinol - Overview of Esterillos, Quepos, & Parrita blocks

The Quepos-Parrita coastal piedmont (Fig. 28) of central Costa Rica consists of a low-relief embayment in the coastal mountain front where the Terraba thrust belt merges with the northern Cordillera de Talamanca. This area encompasses the Parrita and Quepos coastal fault blocks southeast of the Herradura and Esterillos blocks (Fig. 28; Fisher et al., 1994 and 1998; Sak, 1999). Drainage networks (Fig. 3, sites 6-7) developed across the low-lying Parrita block (Fig. 3, site 7; ríos Cañas, Paquita, Naranjo, and Savegre) are deflected by active tectonic uplift around the coastal headland of the smaller Quepos block. This uplift is expressed by the deformation of a flight of four Quaternary terraces formed along these river valleys (Fig. 14; Wells et al., 1988; Drake, 1989). Localized rapid uplift at Quepos may reflect the initial impact of a newly subducting seamount on the coastal fore arc in this area.

A suite of four late Quaternary fluvial terraces occur along the SE margin of the Esterillos block (Fig. 31; Sak, 1999) at elevations up to 185 m above the fault-controlled Río Parrita valley (Fig. 3, site 6). These aggradational gravel deposits are correlated across the Parrita fault with low-lying

terraces on the Parrita block (Sak, 1999). The regional El Diablo surface shows over 150 m of vertical displacement across the Parrita fault (Fig. 15), suggesting that the low-lying Parrita block has an uplift rate an order of magnitude slower than the Esterillos or Herradura blocks to the NW (Fisher et al., 1998). The Parrita terrace deposits extend up to 15 km NW of the modern Río Parrita (Figs. 29 and 31), implying a SE migration of the river channel in response to late Quaternary uplift of the Esterillos block. A NW tilt of the El Diablo surface on both the Esterillos and Parrita blocks (Fig. 15) is consistent with the assymetric drainage patterns observed on both of these blocks. Down-to-the-northwest tilting of the Esterillos and Parrita blocks may reflect the long-wavelength decrease in Cocos plate thickness NW from the Cocos Ridge (Fig. 15). The sharp contrast in uplift rates across the Parrita fault may be due to the short-wavelength effect of seamount subduction beneath the Esterillos and Herradura blocks (Fisher et al., 1998).

Stop 4. Villa Caletas - Overview of Golfo de Nicoya and central Pacific coast

The marvelous view from the ridgetop Villa Caletas hotel encompasses almost the entire area visited during our field trip, including: the Golfo de Nicoya, the southeastern coast of the Península de Nicoya, the Orotina-Esparza coastal plain, and the high rugged mountains of the Herradura headland (Fig. 3). As you look across this spectacular coastal landscape, look also out to sea, and imagine the submarine landscape offshore, with towering seamounts along the rough-smooth boundary, plowing into the depths of the Middle America Trench (Fig. 3). With this picture in mind, you should now have a clear understanding of the dynamic linkage between the subducting seafloor and coastal tectonics along the Costa Rican margin.

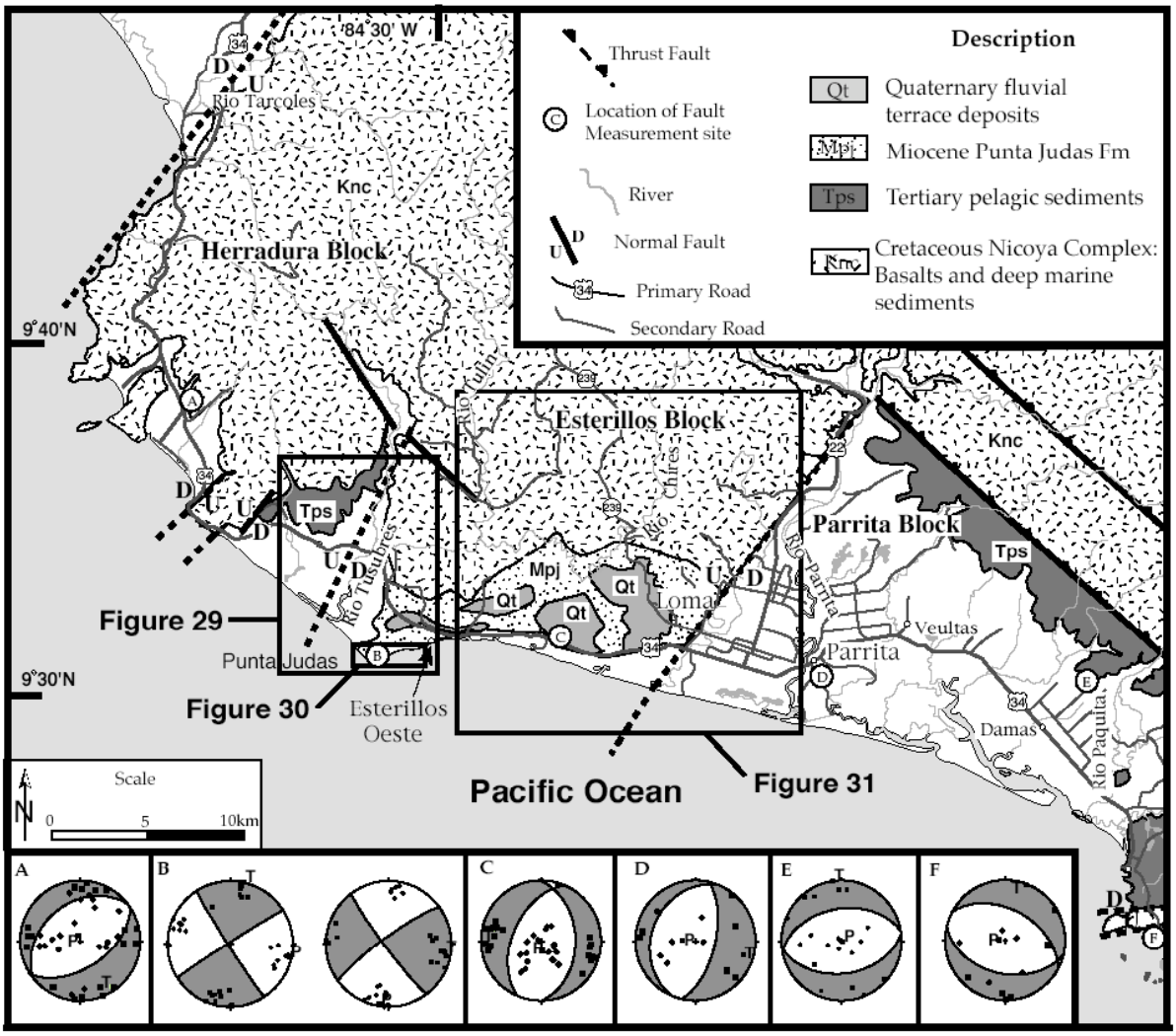

Figure 28. Geologic map spanning the Herradura, Esterillos, Parrita, and Quepos blocks (from Sak, 1999). Mesoscale fault population data (A, C, D, F from Marshall et al., 2000; B, E from Sak, 1999) shown as best fit fault plane solutions (lower hemisphere, equal area) defined by lettered circles. Heavy black lines mark faults with relative vertical displacement indicated by U, up and D, down. Thin light gray lines outline rivers and medium gray lines indicate roads. Rectangles outline areas of Figs. 29, 30, and 31.

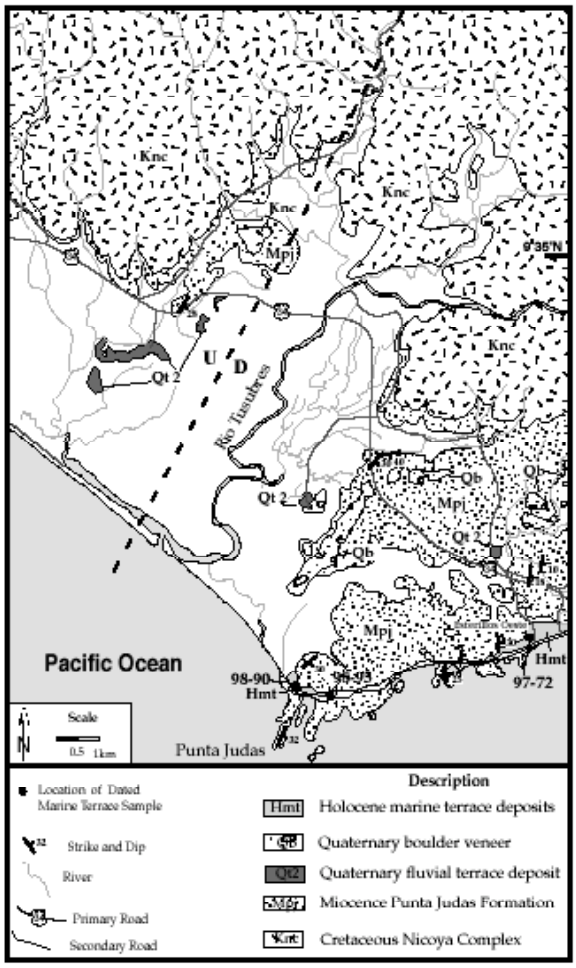

Figure 29. Geologic map of the western Esterillos block (from Sak, 1999) showing the setting of Punta Judas depicted in detail in Fig. 30. See Fig. 28 for location.

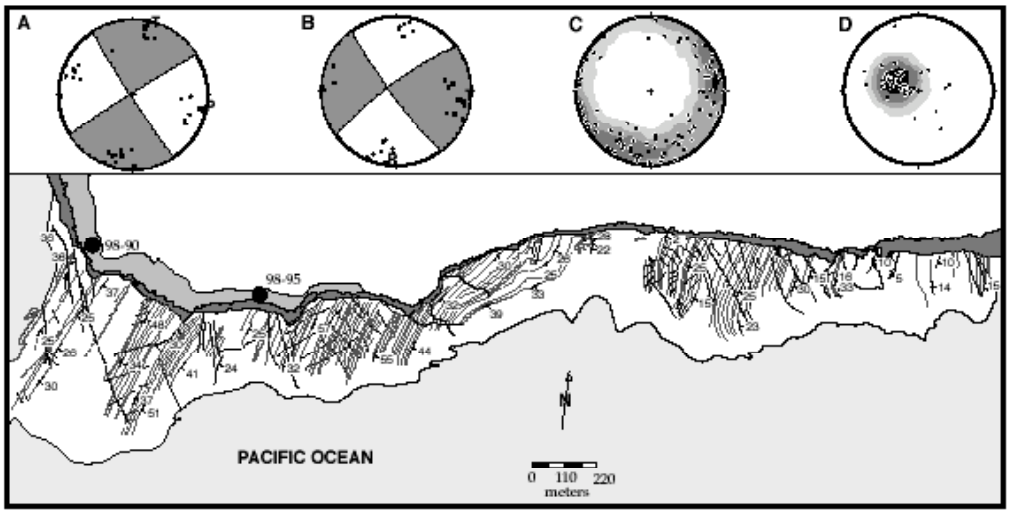

Figure 30. Geologic map (after Haller and Protti, 1987) and structural data (after Sak, 1999) for the wavecut platform at Punta Judas. Active intertidal platform cut in Miocene Punta Judas Fm. shown as white background; modern beach deposits shown in dark gray; uplifted wavecut platform shown in light gray. Black circles show locations of radiocarbon dated samples. Insets A and B show best fit fault plane solutions and kinematic axes for mesoscale fault populations generated by the first (A) and second (B) deformation episodes. Inset C and D show lower hemisphere equal are projections of poles to joints (C) and poles to bedding (D) with superimposed Kamb contour plots.

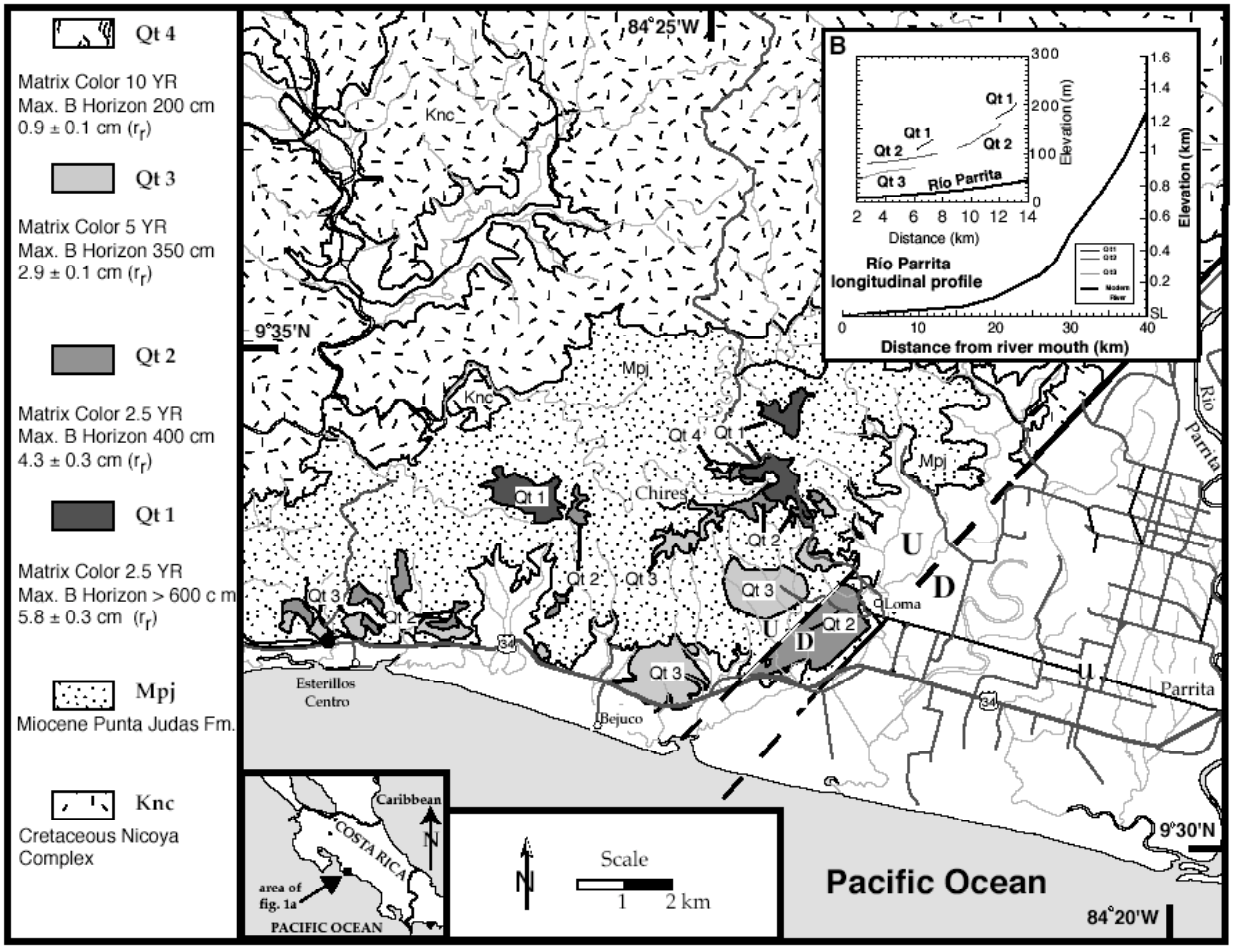

Figure 31. Geologic of the eastern Esterillos block and western Parrita block (from Sak, 1999). showing the distribution of fluvial terraces along the Río Parrita (Fig 3, site 6). Heavy black lines mark faults with relative vertical displacement indicated by U, up and D, down. Thin light gray lines outline rivers and medium gray lines indicate roads. See Fig. 28 for location.

References Cited

Alvarado, G.E., 1985, Consideraciones petrológicas de los estratovolcanes de Costa Rica: Revista Geológica de America Central, v. 3, p. 103-128.

Anderson, R. S., Marshall, J. S., and Brenes Marin, J. A., 1989, Evidence of repeated coseismic uplift along the southern coast of Nicoya peninsula, Costa Rica [abs.]: Geological Society of America Abstracts with Programs, v. 21, p. A 92.

Anderson, R.S., Densmore, A.L., and Ellis, M.A., 1999, The generation and degradation of marine terraces: Basin Research, v. 11, p. 7-19.

Arias, O., 2000, Geología y petrología magmática del Bloque Herradura (Cretácico Superior-Eoceno, Costa Rica), [Ph.D. Thesis]: Lausanne, Switzerland, L'Université de Lausanne, 186 p.

Barckhausen, U., Roeser, H.A., and von Huene, R., 1998, Magnetic signature of upper plate structures and subducting seamounts at the convergent margin off Costa Rica: Journal of Geophysical Research, v. 103, p. 7079-7093.

Battistini, R., and Bergoeing, J.P., 1983, Reconnaissance géomorphologique de la façade Pacifique du Costa Rica: Geomorphologie Littorale, Travaux et Documents de Géographie Tropicale, CEGET, v. 49, 73 p.

Baumgartner, P.O., Mora, C.R., Butterlin, J., Sigal, J., Glacon, G., Azema, J., and Bourgois, J., 1984, Sedimentación y paleogeografía del Cretácio y Cenozóico del litoral Pacífico de Costa Rica: Revista Geológica de América Central, v. 1, p. 57-136.

Bergoeing, J.P., Malavassi, E., and Jimenez, R., 1980, Sintesis geológica del Valle Central de Costa Rica (mapa): San José, Costa Rica, Universidad de Costa Rica (UCR) - Departamento de Geografía, and Ministerio de Obras Públicas y Transporte (MOPT) - Instituto Geográfico Nacional (IGN), 2 p.

Bloom, A.L., and Yonekura, N., 1990, Graphic analysis of dislocated Quaternary shorelines, *in* Geophysics Study Committee, eds., Sea Level Change: Washington, D.C., National Acadamy Press, p. 104-115.

Blum, M.D., and Törnqvist, T.E., 2000, Fluvial responses to climate and sea-level change: a review and look forward: Sedimentology, v. 47, p. 2-48.

Bourgois, J., Azema, J., Baumgartner, P.O., Tournon, J., Desmet, A., and Aubouin, J., 1984, The geologic history of the Caribbean-Cocos plate boundary with special reference to the Nicoya ophiolite complex (Costa Rica) and D.S.D.P. results (legs 67 and 84) off Gautemala: A synthesis: Tectonophysics, v. 108, p. 1-32.

Bull, W.B., 1985, Correlation of flights of global marine terraces, *in* Morisawa, M., and Hack, J.T., eds., Tectonic Geomorphology: Proceedings of the 15th Geomorphology Symposia Series, Binghamton, p. 129-152.

Bullard, T.F., 1995, Neotectonics, geomorphology, and late Quaternary geology across a fore-arc region impacted by the subduction of the aseismic Cocos Ridge, Pacific coast of Costa Rica [Ph.D. thesis]: Albuquerque, New Mexico, University of New Mexico, 775 p.

Burbach, G.V., C. Frohlich, W.D. Pennington, and T. Matumoto, 1984, Seismicity and tectonics of the subducted Cocos Plate: Journal of Geophysical Research, v. 89, p. 7719-7735.

Carr, M.J., 1976, Underthrusting and Quaternary faulting in Central America: Geological Society of America Bulletin, v. 87, p. 825-829.

Calvo, C., 1983, Geología de Cabuya y la parte este de la Reserva Natural Absoluta de Cabo Blanco, Costa Rica [Informe Final, Campaña Geológica]: San José, Costa Rica, Escuela Centroamericana de Geología, Universidad de Costa Rica, 41 p.

Chappell, J., and Polach, H., 1991, Post-glacial sea-level rise from a coral record at Huon Peninsula, Papua New Guinea: Nature, v. 349, p. 147-149.

Chinchilla, A. L., 1983, Geología del area de Montezuma y alrededores, Península de Nicoya, Provincia de Puntarenas, Costa Rica [Informe Final, Campaña Geológica]: San José, Costa Rica, Escuela Centroamericana de Geología, Universidad de Costa Rica, 50 p.

Collins, L.S., Coates, A.G., Jackson, J.B.C., and Obando, J.A., 1995, Timing and rates of emergence of the Limón and Bocas del Toro basins: Caribbean effects of Cocos Ridge subduction?: *in* Mann, P. editor, Geological Society of America Special Paper, No. 295, Geologic and Tectonic Development of the Caribbean Plate Boundary in Southern Central America, p. 291-307.

Corrigan, J., Mann, P., and Ingle, J.C., 1990, Forearc response to subduction of the Cocos Ridge, Panama-Costa Rica: Geological Society of America Bulletin, v. 102, p. 628-652.

de Boer, J., 1979, The outer arc of the Costa Rica orogen (oceanic basement complexes of the Nicoya and Santa Elena peninsulas): Tectonophysics, v. 56, p. 221-259.

de Boer, J.Z., Drummond, M.S., Bordelon, M.J., Defant, M.J., Bellon, H., and Maury, R.C., 1995, Cenozoic magmatic phases of the Costa Rican island arc (Cordillera de Talamanca): *in* Mann, P., ed., Geological Society of America Special Paper, No. 295, Geologic and Tectonic Development of the Caribbean Plate Boundary in Southern Central America, p. 35-55.

De Mets, C., Gordon, R.G., Argus, D.F., and Stein, S., 1990, Current plate motions, Geophysical Journal International, v. 101, p. 425-478.

Dengo, G., 1962, Estudio geológico de la región de Guanecaste, Costa Rica: San José, Costa Rica, Instituto Geográfico Nacional, Costa Rica, 113 p.

Denyer, P., and Arias, O. , 1991, Estratigrafía de la región central de Costa Rica: Revista Geológica de America Central, v. 12, p. 1-59.

Di Marco, G., Baumgartner, P.O., and Channell, J.E.T., 1995, Late Cretaceous-early Tertiary paleomagnetic data and a revised tectonostratigraphic subdivision of Costa Rica and western Panama: *in* Mann, P., ed., Geological Society of America Special Paper, No. 295, Geologic and Tectonic Development of the Caribbean Plate Boundary in Southern Central America, p. 1-27.

Dondoli, C., 1958, Breve reseña geológica, *in* Leitón, J.S. and Sáenz, R., Estudio semidetallado de los suelos de la región comprendida entre los ríos Barranca y Lagarto, Minesterio de Agricultura e Industrias, Boletín Tecnico, 24, p.15-18.

Donnelly, T. W., 1994, The Caribbean Cretaceous basalt association: A vast igneous province that includes the Nicoya complex of Costa Rica, in Seyfried, H. and Hellmann, W., eds., Profil 7, Geology of an evolving island arc: Stuttgart, Universität Stuttgart, p. 17-45.

Drake, P.G., 1989, Quaternary geology and tectonic geomorphology of the coastal piedmont and range, Puerto Quepos area, Costa Rica [M.S. thesis]: Albuquerque, New Mexico, University of New Mexico, 183 p.

Echandi, E., 1981, Unidades volcánicas de la vertiente norte de la cuenca del río Virilla, [Tesis de Licenciatura], Escuela Centroamericana de Geológia, Universidad de Costa Rica, San José, 123 p.

Fairbanks, R. G., 1989, A 17,000-year glacio-eustatic sea level record: influence of glacial melting rates on the Younger Dryas event and the deep-ocean circulation: Nature, v. 342, p. 637-642.

Fisher, D.M., Gardner, T.W., Marshall, J.S., and Montero, W., 1994, Kinematics associated with late Tertiary and Quaternary deformation in central Costa Rica: Western boundary of the Panama microplate: Geology, v. 22, p. 263-266.

Fisher, D.M., Gardner, T.W., Marshall, J.S., Sak, P.B., and Protti, M., 1998, Effect of subducting sea-floor roughness on fore-arc kinematics, Pacific coast, Costa Rica: Geology, v. 26, p. 467-470.

Fischer, R., 1980, Recent tectonic movements of the Costa Rican Pacific coast: Tectonophysics, v. 70, p. T25-T33.

Gardner, T.W., Back, W., Bullard, T.F., Hare, P., Kesel, R.H., Lowe, D.R., Menges, C.M., Mora, S.C., Pazzaglia, F.J., Sasowsky, I.R., Troester, J.W., and Wells, S.G., 1987, Central America and the Caribbean: *in* Graf, W. L., ed., Geomorphic systems of North America: Geologic Society of America, Centennial Special Volume 2, p. 343-402.

Gardner, T.W., Verdonck, D., Pinter, N.M., Slingerland, R., Furlong, K.P., Bullard, T.F., and Wells, S.G., 1992, Quaternary uplift astride the aseismic Cocos Ridge, Pacific coast, Costa Rica: Geological Society of America Bulletin, v. 104, p. 219-232.

Gardner, T.W., Fisher, D.M., and Marshall, J.S., 1993, Western boundary of the Panama microplate, Costa Rica: Geomorphological and structural constraints [abs.]: International Association of Geomorphologists, Third International Geomorphology Conference, McMaster University, Hamilton, Ontario, Canada, Programme with Abstracts, p. 143.

Gardner, T., Marshall, J., Merritts, D., Protti, M., Bee, B., Burgette, R., Burton, E., Cooke, J., Kehrwald, N., Fisher, D., and Sak, P., 2001, Holocene fore arc block rotation in response to seamount subduction, southeastern Península de Nicoya, Costa Rica: Geology, v. 29, no. 2, p. 151-154.

Gardner, T.W., Fisher, D.M., Marshall, J.S., and Sak, P., 2000, Fore arc deformation, segmentation, and drainage evolution in response to seamount subduction along an eroding margin, Pacific coast, Costa Rica [abs.]: Eos, Proceedings of the Amererican Geophysical Union, v.81, no. 48, p. F1206.

Gerth, R.A., 2000, La Boquita terrace, Nicaragua: Evidence for uplift of the central Pacific coast, [M.S. thesis]: Santa Cruz, California, University of California, Santa Cruz, 85 p.

Gerth, R., Silver, E., Marshall, J., Duarte, M., Carr, M., McIntosh, K., Strauch, W., Sweet, S., Kling, S., and Protti, M., 1999, La Boquita terrace, Nicaragua: Evidence for uplift of the central Pacific coastal zone [abs.]: Eos, Proceedings of the Amererican Geophysical Union, v.80, no. 46, p. F1033.

González-Víquez, C., 1910, Temblores, terremotos, inundaciones y erupciones volcánicas en Costa Rica, 1608-1910: San José, Costa Rica, Tipografía de Avelino Alsina, 200 p.

Güendel, F., 1986, Seismotectonics of Costa Rica: An analytical view of the southern terminus of the Middle America Trench [PhD dissertation]: Santa Cruz, California, University of California, Santa Cruz, 157 p.

Güendel, F., Montero, C., Rojas, D., Brenes, J., Segura, J., Sáenz, R., and González, V., 1989, Informe sobre el enjambre sismico ocurrido cerca de la cuidad de Orotina entre el 21 y el 24 de Enero de 1989: Boletín Sismológico, Observatorio Vulcanológico y Sismológico de Costa Rica, v. 5, p. 9-16.

Haller, D.F., and Protti, J.M., 1987, Local and regional aspects of structural geology: Punta Judas, Puntarenas, Costa Rica [Senior Thesis]: Associated Colleges of the Midwest, 42 p.

Hare, P.W., and Gardner, T.W., 1985, Geomorphic indicators of vertical neotectonism along converging plate margins, Nicoya Peninsula, Costa Rica, *in* Morisawa, M., and Hack, J.T., eds., Tectonic geomorphology: Proceedings of the 15th Geomorphology Symposia Series, Binghamton, p. 76-104.

Hey, R., 1977, Tectonic evolution of the Cocos-Nazca spreading center: Geological Society of America Bulletin, v. 88, p. 1404-1420.

Hill, R.T., 1898, The geological history of the isthmus of Panama and a portion of Costa Rica: Bulletin of the Museum of Comparative Zoology, Harvard College, v. 28 (5), 285 p.

Hinz, K., von Huene, R., Ranero, C.R., and the PACOMAR working group, 1996, Tectonic structure of the convergent Pacific margin offshore Costa Rica from multichannel seismic reflection data: Tectonics, v. 15, p. 54-66.

Holden, J.C., and Dietz, R.S., 1972, Galapagos gore, NazCoPac triple junction and Carnegie/Cocos ridges: Nature, v. 235, p. 266-269.

Imbrie, et al., 1984, The orbital theory of Pleistocene climate: Support from a revised chronolgy of the marine $\delta^{18}O$ record: *in* Berger, A., ed., Milankovitch and Climate, Dordrect, Netherlands, D. Reidel, p. 269-305.

Jarrard, R. D., 1986, Relations among subduction parameters: Reviews of Geophysics, v. 24, p. 217-284.

Kellogg, J.N., and V. Vega, 1995, Tectonic development of Panama, Costa Rica, and the Colombian Andes: Constraints from global positioning system geodetic studies and gravity: *in* Mann, P., ed., Geological Society of America Special Paper, No. 295, Geologic and Tectonic Development of the Caribbean Plate Boundary in Southern Central America, p. 75-90.

Kesel, R.H., and Spicer, B.E., 1985, Geomorphologic relationships and ages of soils on alluvial fans in the Río General valley, Costa Rica: Catena, v. 12, p. 149-166.

Kimura, G., Silver, E.A., Blum, P., et al., 1997. Proceedings of the Ocean Drilling Program, Initial Reports, v. 170: College Station, TX (Ocean Drilling Program).

Kolarsky, R.A., Mann, P., and Montero, W., 1995, Island arc response to shallow subduction of the Cocos Ridge, Costa Rica: *in* Mann, P., ed., Geological Society of America Special Paper, No. 295, Geologic and Tectonic Development of the Caribbean Plate Boundary in Southern Central America, p. 235-262.

Kruckow, T., 1974, Landhebung im Valle Central und Wachstum der Küstenebenen in Costa Rica (Mittelamerika): Jahrbuch der Wittheit zu Bremen, v. 18, p. 247-263.

Kuijpers, E. P., 1980, The geologic history of the Nicoya ophiolite complex, Costa Rica, and its geotectonic significance: Tectonophysics, v. 68, p. 233-255.

Kussmaul, S., Tournon, J., and Alvarado, G., 1994, Evolution of the Neogene to Quaternary igneous rocks of Costa Rica: Profil, Institut für Geologie und Palaontologie, Universität Stuttgart, v. 7, p. 97-123.

Lajoie, K. R., 1986, Coastal tectonics: *in* Active Tectonics,Washington, D. C., National Acadamy Press, p. 95-124.

Lonsdale, P., and Klitgord, K.D., 1978, Structure and tectonic history of the eastern Panama basin: Geological Society of America Bulletin, v. 89, p. 981-999.

Lundberg, N., 1982, Evolution of the slope landward of the Middle America Trench, Nicoya Peninsula, Costa Rica, *in* Legget, J. K., ed., Trench-forearc geology: Geological Society of London Special Publication 10, p. 131-147.

Lundberg, N., 1991, Detrital record of the early Central American magmatic arc: Petrography of intraoceanic forearc sandstones, Nicoya Peninsula, Costa Rica: Geological Society of America Bulletin, v.103, p. 905-915.

Mackay, M.E., and Moore, G.F., 1990, Variation in deformation of the south Panama accretionary prism: Response to oblique subduction and trench sediment variation: Tectonics, v. 9, p. 683-698.

Madrigal, R., 1970, Geología del mapa básico Barranca, Costa Rica: Ministerio de Industia y Comercio, Informes Técnicos y Notas Geológicas, no. 37, San José, Costa Rica, 55 p.

Malavassi, E., 1991, Magma sources and crustal processes at the southern terminus of the Middle American volcanic arc [PhD dissertation]: Santa Cruz, California, University of California, Santa Cruz.

Marshall, J.S., 1991, Neotectonics of the Nicoya Peninsula, Costa Rica: A look at forearc response to subduction at the Middle America Trench [M.S. thesis]: Santa Cruz, California, University of California, Santa Cruz, 196 p.

Marshall, J.S., 2000, Active tectonics and Quaternary landscape evolution across the western Panama block, Costa Rica, Central America, [Ph.D. Thesis]: University Park, Pennsylvania State University, 304 p.

Marshall, J.S., and Anderson, R.S., 1995, Quaternary uplift and seismic cycle deformation, Península de Nicoya, Costa Rica: Geological Society of America Bulletin, v. 107, p. 463-473.

Marshall, J.S., and Idleman, B.D., 1999, $^{40}Ar/^{39}Ar$ age constraints on Quaternary landscape evolution of the central volcanic arc and Orotina debris fan, Costa Rica [abs.]: Geological Society of America Abstracts with Programs, v. 31, p. A479.

Marshall, J.S., Fisher, D.M., and Gardner, T.G., 2000, Central Costa Rica deformed belt: Kinematics of diffuse faulting across the western Panama block: Tectonics, v. 19, p. 468-492.

McIntosh, K., Silver, E., and Shipley, T., 1993. Evidence and mechanisms for fore-arc extension at the accretionary Costa Rica convergent margin: Tectonics, v. 12, p. 1380-1392.

Merritts, D.J., Vincent, K.R., and Wohl, E.E., 1994, Long river profiles, tectonism, and eustasy: a guide to interpreting fluvial terraces: Journal of Geophysical Research, v. 99, p. 14031-14050.

Meschede, M., Barckhausen, U., and Worm, H.U., 1998, Extinct spreading on the Cocos Ridge: Terra Nova, v. 10, p. 211-216.

Meschede, M., Zweigel, P., and Kiefer, E., 1999a, Subsidence and extension at a convergent margin: Evidence for subduction erosion off Costa Rica, Terra Nova, v. 11, p. 112-117.

Meschede, M., Zweigel, P., Frisch, W., and Völker, D., 1999b, Mélange formation by subduction erosion: The case of the Osa mélange in southern Costa Rica: Terra Nova, v. 11, p. 141-148.

Ministerio de Industria, Energia y Minas, 1982, Mapa Geológico de Costa Rica, scale 1:200,000, sheets CR2CM-4, 5, 6, 7, and 8, San José, Costa Rica.

Montero, W., 1994, Neotectonics and related stress distribution in a subduction-collisional zone: Costa Rica: *in* Seyfried, H. and Hellmann, W., eds., Profil 7, Geology of an evolving island arc: Stuttgart, Universität Stuttgart, p. 126-141.

Mora, C.R., 1985, Sedimentología y geomorfología del sur de la Península de Nicoya (Provincia de Puntarenas, Costa Rica) [Tesis de Licenciatura]: San José, Costa Rica, Escuela Centroamericana de Geológia, Universidad de Costa Rica, 148 p.

Nishenko, S. P., 1989, Circum-Pacific seismic potential, 1989-1999: U. S. Geological Survey Open-File Report 89-86.

Pazzaglia, F.J., Gardner, T.W., and Merritts, D.J., 1998, Bedrock incision and longitudinal profile development over geologic time scales determined by fluvial terraces: *in* Whol, E. and Tinkler, K., eds., American Geophysical Union Monograph Series No. 107, Rivers Over Rock: Fluvial Processes in Bedrock Channels, p. 207-236.

Pinter, N., 1988, Isostasy and eustasy on the Osa Peninsula, Costa Rica: Unraveling the late Quaternary geologic history through uplift and sea level change [M.S. thesis]: University Park, Pennsylvania, Pennsylvania State University, 144 p.

Protti, J. M., 1991, Correlation between the age of the subducting Cocos Plate and the geometry of the Wadati-Benioff zone under Nicaragua and Costa Rica [M.S. thesis]: Santa Cruz, California, University of California, Santa Cruz, 66 p.

Protti, J. M., 1994, The most recent large earthquakes in Costa Rica (1990, M_W = 7.0 and 1991, M_W = 7.6) and three-dimensional crustal and upper mantle P-wave velocity structure of central Costa Rica [PhD dissertation]: Santa Cruz, California, University of California, Santa Cruz, 116 p.

Protti, M., and S.Y. Schwartz, 1994, Mechanics of back arc deformation in Costa Rica: Evidence from an aftershock study of the April 22, 1991, Valle de la Estrella, Costa Rica, earthquake (M_W=7.7): Tectonics, v. 13, p. 1093-1107.

Protti, M., Güendel, F., and McNally, K., 1995, Correlation between the age of the subducting Cocos plate and the geometry of the Wadati-Benioff zone under Nicaragua and Costa Rica: *in* Mann, P. editor, Geological Society of America Special Paper, No. 295, Geologic and Tectonic Development of the Caribbean Plate Boundary in Southern Central America, p. 309-326.

Sak, P.B., 1999, Landscape evolution and structure of the central Pacific coast, Costa Rica [M.S. thesis]: University Park, Pennsylvania, Pennsylvania State University, 44 p.

Sak, P.B., Fisher, D.M., Gardner, T.W., and Brantley, S.L., in review, Diffusion models for weathering rind genesis in a tropical setting: submitted to Geochimica et Cosmochimica Acta.

Seyfried, H., Krawinkel, H., and Aguilar, T., 1994, Significance of stratigraphic bounding surfaces in a shallow marine, sand-swamped forearc basin: A cas study from the Punta Judas Formation (Miocenc, Costa Rica): *in* Seyfried, H. and Hellmann, W., eds., Profil 7, Geology of an evolving island arc: Stuttgart, Universität Stuttgart, p. 293-323.

Shackleton, N.J., and Opdyke, N.D., 1973, Oxygen isotope and palaeomagnetic stratigraphy of equatorial Pacific core V28-238: Oxygen isotope temperatures and ice volumes on a 10^5 year and 10^6 year scale: Quaternary Research, v. 3, p. 39-55.

Shipley, T. H., McIntosh, K. D., Silver, E. A., and Stoffa, P. L., 1992, Three-dimensional seismic imaging of the Costa Rica accretionary prism: structural diversity in a small volume of the lower slope: Journal of Geophysical, Research, v. 97, p. 4439-4459.

Silver, E.A., Reed, D.L., Tagudin, J.E., and Heil, D.J., 1990, Implications of the north and south Panama thrust belts for the origin of the Panama orocline: Tectonics, v. 9, p. 261-281.

Sinton, C.W., Duncan, R.A., and Denyer, P., 1997, Nicoya Peninsula, Costa Rica: A single suite of Caribbean oceanic plateau magmas: Journal of Geophysical Research, v. 102, No. B7, p. 15,507-15,520.

Stavenhagen, A.U., Flueh, E.R., Ranero, C., McIntosh, K.D., Shipley, T., Leandro, G., Schulze, A., and Dañobeitia, J.J., 1998, Seismic wide-angle investigations in Costa Rica: A crustal velocity model from the Pacific to the Caribbean coast: Zentralblat für Geologie und Palaeontologie, Teil I, v. 3-6, p. 393-408.

Stoffa, P. L., Shipley, T. H., Dean, D. F., Kessinger, W. K., Elde, R., Silver, E., Reed, D., and A. Aguilar, 1991, Three-dimensional seismic imaging of the Costa Rica accretionary wedge: field program and migration examples: Journal of Geophysical Research, v. 96, p. 21693-21712.

Stoiber, R.E., and Carr, M., 1973, Quaternary volcanic and tectonic segmentation of Central America, Bulletin of Volcanology, v. 37, p. 304-325.

Talling, P.J., 1998, How and where do incised valleys form if sea-level remains below the shelf edge?: Geology, v. 26, p. 87-90.

Vannuchi, Scholl, D., Meschede, M., 2000, Subduction erosion as the major process controlling the evolution of the Costa Rica sector of the Middle America Trench: Leg 170 drilling results and coastal studies of the adjacent Nicoya Peninsula [abs.]: Eos, Proceedings of the Amererican Geophysical Union, v.81, no. 48, p. F1179.

von Huene, R. and Flüh, E., 1994, A review of marine geophysical studies along the Middle America Trench off Costa Rica and the problematic seaward terminus of continental crust: *in* Seyfried, H. and Hellmann, W., eds., Profil 7, Geology of an evolving island arc: Stuttgart, Universität Stuttgart, p. 143-160.

von Huene, R. and 16 others, 1995, Morphotectonic features of the Pacific convergent margin of Costa Rica: *in* Mann, P., ed., Geological Society of America Special Paper, No. 295, Geologic and Tectonic Development of the Caribbean Plate Boundary in Southern Central America, p. 291-307.

von Huene, R., Ranero, C., Weinrebe, W., and Hinz, K., 2000, Quaternary convergent margin tectonics of Costa Rica: segmentation of the Cocos Plate and Central American volcanism: Tectonics, v.19, p. 314-334.

Wells, S.G., Bullard, T.F., Menges, C.M., Drake, P.G., Karas, P.A., Kelson, K.I., Ritter, J.B., and Wesling, J.R., 1988, Regional variations in tectonic geomorpholgy along a segmented convergent plate boundary, Pacific coast of Costa Rica: Geomorphology, v. 1, p. 239-265.

Werner, R., Hoernle, K., van den Bogaard, P., Ranero, C., von Huene, R., and Korich, D., 1999, Drowned 14 m.y. old Galápagos archipelago off the coast of Costa Rica: Implications for tectonic and evolutionary models: Geology, v. 27, p. 499-502.

Westbrook, G.K., Hardy, N.C., and Heath, R.P., 1995, Structure and tectonics of the Panama-Nazca plate boundary: *in* Mann, P., ed., Geological Society of America Special Paper, No. 295, Geologic and Tectonic Development of the Caribbean Plate Boundary in Southern Central America, p. 91-109.

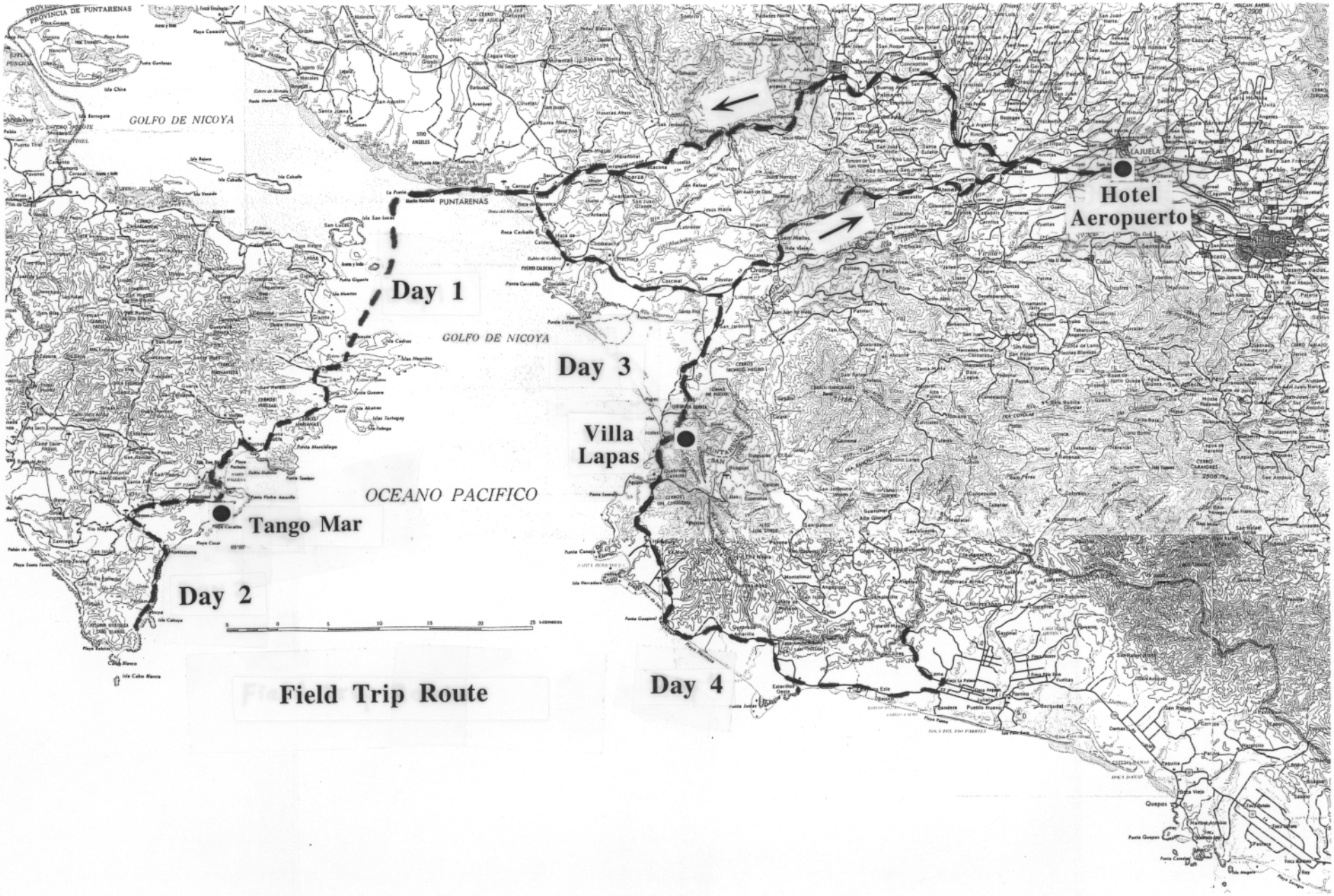
GOLFO DE NICOYA
PUNTARENAS
Day 1
GOLFO DE NICOYA
Day 3
Villa Lapas
OCEANO PACIFICO
Tango Mar
Day 2
Hotel Aeropuerto
Day 4
Field Trip Route

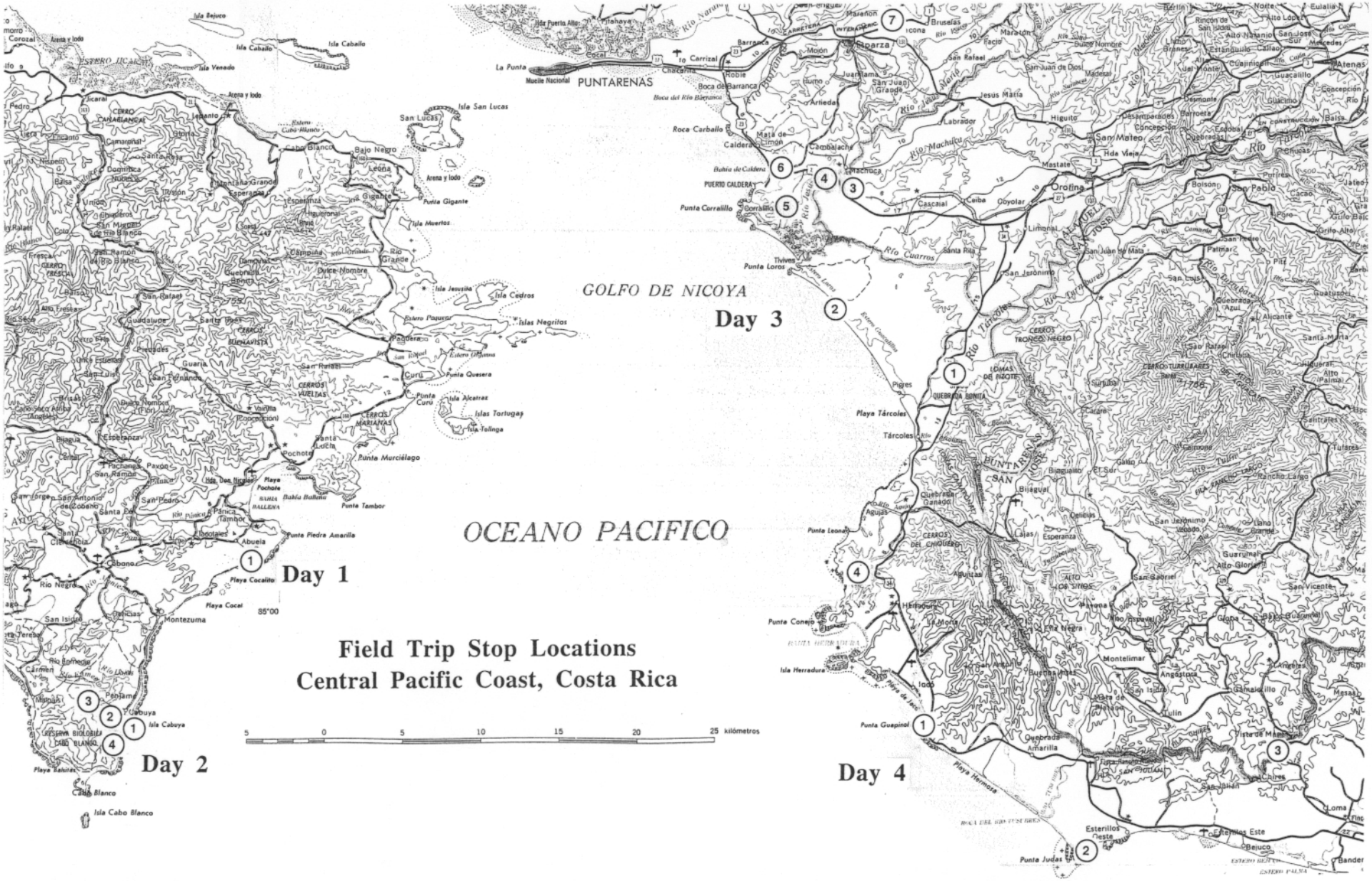
PUNTARENAS
GOLFO DE NICOYA
OCEANO PACIFICO
Day 1
Day 2
Day 3
Day 4
Field Trip Stop Locations
Central Pacific Coast, Costa Rica
5 0 5 10 15 20 25 kilómetros